PAPER

On dissipative symplectic integration with applications to gradient-based optimization

Journal of Statistical Mechanics: Theory and Experiment
An IOP and SISSA journal

PAPER: Interdisciplinary statistical mechanics

On dissipative symplectic integration with applications to gradient-based optimization

Guilherme França[1,2,*], **Michael I Jordan**[1] **and René Vidal**[2]

[1] University of California, Berkeley, CA 94720, United States of America
[2] Johns Hopkins University, Baltimore, MD 21218, United States of America
E-mail: guifranca@gmail.com

Received 25 June 2020
Accepted for publication 13 March 2021
Published 26 April 2021

Online at stacks.iop.org/JSTAT/2021/043402
https://doi.org/10.1088/1742-5468/abf5d4

Abstract. Recently, continuous-time dynamical systems have proved useful in providing conceptual and quantitative insights into gradient-based optimization, widely used in modern machine learning and statistics. An important question that arises in this line of work is how to discretize the system in such a way that its stability and rates of convergence are preserved. In this paper we propose a geometric framework in which such discretizations can be realized systematically, enabling the derivation of 'rate-matching' algorithms without the need for a discrete convergence analysis. More specifically, we show that a generalization of symplectic integrators to non-conservative and in particular dissipative Hamiltonian systems is able to preserve rates of convergence up to a controlled error. Moreover, such methods preserve a shadow Hamiltonian despite the absence of a conservation law, extending key results of symplectic integrators to non-conservative cases. Our arguments rely on a combination of backward error analysis with fundamental results from symplectic geometry. We stress that although the original motivation for this work was the application to optimization, where dissipative systems play a natural role, they are fully general and not only provide a differential geometric framework for dissipative Hamiltonian systems but also substantially extend the theory of structure-preserving integration.

*Author to whom any correspondence should be addressed.

1742-5468/21/043402+39$33.00

Keywords: machine learning, optimization under uncertainty, analysis of algorithms

Contents

1. Introduction

A recent line of research at the interface of machine learning and optimization focuses on establishing connections between continuous-time dynamical systems and gradient-based optimization methods [1–13]. From this perspective, an optimization algorithm corresponds to a particular discretization of a differential equation. Moreover, important *accelerated methods* such as Nesterov's method [14] and Polyak's heavy ball method [15] are modeled as second-order differential equations with a dissipative term [1–5]. There are advantages to working in continuous time. In particular, the stability and convergence analysis of a continuous-time system tends to be simpler and more transparent, making use of general tools such as Lyapunov stability theory and variational formulations. The traditional discrete analysis is usually only applicable on a case-by-case basis and often requires painstaking algebra. This is an unsatisfactory state of affairs given that accelerated optimization methods are the workhorses behind many of the empirical success stories in large-scale machine learning.

A particularly useful step has been the development of a variational perspective on acceleration methods [2]. This framework, which involves the definition the so-called *Bregman Hamiltonian*, places momentum-based methods such as Nesterov acceleration into a larger class of dynamical systems and has accordingly helped to demystify the notion of 'acceleration' in an optimization context. Two difficulties arise, however, when one attempts to further exploit and characterize this class of systems. First, there are many different ways to discretize a continuum system. A naive discretization may be unable to preserve rates of convergence—i.e. rates of decay to lower-energy level sets—and may even lead to an unstable algorithm. Moreover, it is largely unknown if there exists an underlying principle from which one can construct such 'rate-matching' discretizations. Thus a fundamental question arises:

> *Which classes of discretizations are capable of preserving the rates of convergence of the continuous-time dynamical systems of interest in optimization?*

A second difficulty is that the Hamiltonian formalism has traditionally been applied to conservative systems; in particular, systems characterized by oscillations. Such behavior is incommensurate with the desire to converge to an optimum—a system that converges towards a limit cycle may have favorable stability properties, but the presence of limit cycles may preclude convergence to a point. Thus we have a second fundamental question:

> *Can we map discrete-time algorithms into dissipative continuous-time dynamical systems that provide analytical insight into the behavior of the original algorithm?*

Clearly these two questions are related. Indeed, the ability to map between dynamical systems while preserving rates may be seen as a form of 'invariance'—although different from the conservation laws arising from Noether's theorem.

In this paper we attempt to provide answers to the above questions. Introducing a class of *dissipative Hamiltonian systems*, we combine fundamental results from symplectic geometry [16, 17] and backward error analysis [18–20] to establish a general quantitative guarantee for the convergence of discrete algorithms based on these continuum dynamics. More specifically, we propose a class of discretizations, which we refer

J. Stat. Mech. (2021) 043402

to as *presymplectic integrators*, that are designed to preserve a fundamental geometric structure associated with non-conservative, and in particular dissipative, Hamiltonian systems[3].

Presymplectic integrators consist of a generalization of the well-known family of *symplectic integrators* [21–25] which have been developed in the setting of *conservative* Hamiltonian systems. The most important property of symplectic integrators is that in addition to preserving the symplectic structure, they exactly conserve a perturbed or shadow Hamiltonian [18], thus ensuring long-term stability. This crucial result relies on the fact that the Hamiltonian is a constant of motion. On the other hand, there are relatively few results on structure-preserving methods for dissipative systems, although this has been the subject of a nascent literature [26–31]. It is thus unknown if the key stability properties of symplectic integrators can be extended to dissipative cases precisely because a conserved quantity is no longer available. We will show that presymplectic integrators allow such properties to be extended into a non-conservative setting. In particular, we show that they preserve a (time-dependent) shadow Hamiltonian and accordingly exhibit long-term stability. Our argument relies on a *symplectification* procedure where the non-conservative system is embedded in the phase space of a higher-dimensional conservative system.

Although the principal goal of our work is to bring a dissipative physical systems perspective to gradient-based optimization, we note that our results are fully general and not tied to applications to optimization; rather, they yield a general differential-geometric framework for the study of non-autonomous and dissipative Hamiltonian systems. They also extend the existing theory of structure-preserving integration to such cases. Our approach may therefore be of interest in other fields where the simulation of dissipative systems is important, such as out-of-equilibrium statistical mechanics, thermodynamics of open systems, complex systems, nonlinear dynamics, etc.

This paper is organized as follows. In appendix A we introduce notation and recall the basic concepts from differential geometry that are needed throughout the paper. In section 2 we provide a high level overview of the main outline of our analysis with a focus on the implications to optimization. Section 3 introduces ideas from backward error analysis and symplectic integrators (for conservative systems), presenting independent geometric proofs of earlier results [18–20] so as to anticipate our generalizations to dissipative systems. In section 4 we introduce non-conservative Hamiltonian systems from the point of view of symplectic geometry and construct their symplectification. We then define presymplectic integrators and argue that they extend the useful properties of symplectic integrators into non-conservative settings. In section 5 we consider the implications of this framework for preserving convergence rates and stability of dissipative Hamiltonian systems, which in particular justify this approach for solving optimization problems. In section 6 we construct explicit presymplectic integrators for the Bregman Hamiltonian in full generality. In section 7 we provide numerical evidence that support our theoretical results. Section 8 contains our final remarks.

[3] This will be made precise later but briefly the idea is that the phase space of a non-conservative Hamiltonian system is a *presymplectic manifold*, endowed with a closed *degenerate* symplectic two-form, which is exactly preserved by a presymplectic integrator.

J. Stat. Mech. (2021) 043402

2. Overview of the implications to accelerated optimization

Given an n-dimensional smooth manifold $\mathcal{M}$ and a function $f:\mathcal{M}\to\mathbb{R}$, consider the optimization problem

$$f(q^\star)=\min_{q\in\mathcal{M}} f(q). \tag{1}$$

Let $H=H(t,q,p)$ be an explicitly *time-dependent* Hamiltonian over the phase space $(q,p)\in T^\star\mathcal{M}$—the cotangent bundle of $\mathcal{M}$ (see appendix A)—which determines dynamical evolution through Hamilton's equations:

$$\frac{\mathrm{d}q^j}{\mathrm{d}t}=\frac{\partial H}{\partial p_j},\qquad \frac{\mathrm{d}p_j}{\mathrm{d}t}=-\frac{\partial H}{\partial q^j}, \tag{2}$$

for $j=1,\dots,n$. We will design dissipative systems whose trajectories tend to a low-energy level set that is consistent with a minimum of f[4]. Specifically, we consider systems arising from the following general family of Hamiltonians:

$$H\equiv \mathrm{e}^{-\eta_1(t)}T(t,q,p)+\mathrm{e}^{\eta_2(t)}f(q), \tag{3}$$

where η_1 and η_2 are positive and monotone increasing functions that are responsible for introducing dissipation. The kinetic energy T is assumed to be Lipschitz continuous. This Hamiltonian includes many dissipative systems that are relevant to optimization, including the Bregman Hamiltonian [2] and conformal Hamiltonian systems [32]—see appendix B for a generalization thereof. Note also that (3) generalizes the Caldirola–Kanai Hamiltonian [33, 34] which can be seen as the classical limit of the seminal Caldeira–Leggett model [35], important in quantum dissipation and decoherence.

It is possible to characterize the convergence rate that a dissipative system tends to a minimum through a Lyapunov analysis [1–3, 7]. This leads to upper bounds of the general form

$$f(q(t))-f(q^\star)=\mathcal{O}\left(\mathcal{R}(t)\right) \tag{4}$$

where $\mathcal{R}(t)$ is a decreasing function of time that depends on the landscape of f. One of our goals is to construct 'rate-matching' discretizations, namely general numerical integrators able to reproduce (4). As previously mentioned, we propose a class of discretizations called presymplectic integrators to this end—this is formalized in definition 8 below.

Let $x\equiv(q,p)$. A numerical integrator for the Hamiltonian system (2) is a map $\phi_h:\mathbb{R}^{2n}\to\mathbb{R}^{2n}$, with step size $h>0$, such that iterations

$$x_\ell=\phi_h(x_{\ell-1}),\qquad x_0=x(0), \tag{5}$$

[4] By way of contrast, a classical conservative system has a *time-independent* Hamiltonian, $H=H(q,p)$, such that $\frac{\mathrm{d}H}{\mathrm{d}t}=0$, implying that trajectories oscillate around a minimum instead of converging.

J. Stat. Mech. (2021) 043402

approximate the true state $x(t_\ell) \equiv (q(t_\ell), p(t_\ell))$ at instants $t_\ell = h\ell$ ($\ell = 1, 2, \ldots$). Let φ_t denote the true flow of (2). An integrator ϕ_h is said to be of *order* $r \geqslant 1$ if

$$\|\phi_h(x) - \varphi_h(x)\| = \mathcal{O}(h^{r+1}), \tag{6}$$

for any $x \in T^*\mathcal{M}$. We also introduce a Lipschitz assumption for the integrator:

$$\|\phi_h(y) - \phi_h(x)\| \leqslant (1 + hL_\phi)\|y - x\| \tag{7}$$

for some constant $L_\phi > 0$ and for all $x, y \in T^*\mathcal{M}$[5]. We now state one of our main results, which we will further explicate and establish formally in the remainder of the paper.

Theorem 1. *Consider a dissipative Hamiltonian system (2) obtained from (3). Let ϕ_h be a presymplectic integrator of order r, assumed to obey the Lipschitz condition (7). Then ϕ_h preserves the continuous rates of convergence up to a small error, namely*

$$\underbrace{f(q_\ell) - f(q^\star)}_{\text{discrete rate}} = \underbrace{f(q(t_\ell)) - f(q^\star)}_{\text{continuous rate}} + \underbrace{\mathcal{O}\left(h^r e^{-\eta_2(t_\ell)}\right)}_{\text{small error}}, \tag{8}$$

provided $e^{L_\phi t_\ell - \eta_1(t_\ell)} < \infty$ for sufficiently large t_ℓ. This holds for exponentially large times $t_\ell \equiv h\ell = \mathcal{O}(h^r e^r e^{h_0/h})$, where the constant $h_0 > 0$ is independent of h.

This theorem shows that presymplectic integration can provide answers to the questions posed earlier regarding the possibility of rate-matching discretizations of dissipative systems. The assumptions of the theorem are mild, and the restriction on t_ℓ may be irrelevant in practice. More importantly, the error in (8) is small and improves with r, though it is dominated by η_2 which suggests that, in this context, higher-order integrators are not likely to be needed. Note that choosing a suitable η_2 is essential since it can make the error negligible; e.g. with $\eta_2 \sim t$ the error is exponentially small.

There is another important aspect of presymplectic integrators worth noting. Since they exactly preserve the phase space geometry, they reproduce the qualitative features of the phase portrait and in particular the stability of critical points. This is not the case for typical discretizations, which in general introduce spurious damping or excitation. In short, given any suitable dissipative system obtained from (3), presymplectic integrators constitute a general approach for the construction of optimization algorithms that are guaranteed to respect the stability and rates of convergence of the underlying dynamical system. We carry out such an approach and consider explicitly the case of the Bregman Hamiltonian in section 6 and also provide general examples in appendix C.

3. Conservative Hamiltonian systems and symplectic integrators

In the remainder of the paper we provide a complete theoretical derivation justifying theorem 1. To build up to that derivation, we first recall several essential concepts from backward error analysis, symplectic geometry, and dynamical systems. These concepts are necessary for an understanding of how one can draw conclusions about

[5] This condition is satisfied by a large class of methods, even including simple ones such as the explicit Euler method which does not preserve any dynamical invariant [21, 22].

J. Stat. Mech. (2021) 043402

structure-preserving methods without a discrete-time analysis. For further background on the basic differential geometry that we use to develop our ideas, we refer the reader to appendix A.

3.1. Numerical integrators and modified equations

Let $\mathcal{M}$ be an n-dimensional smooth manifold, and let $(\mathcal{U}, x)$ be a chart such that every point $p \in \mathcal{U} \subset \mathcal{M}$ has local coordinates $x^1, \ldots, x^n$ in $\mathbb{R}^n$. From now on we refer to a point p by its coordinates x. Given a vector field $X \in T\mathcal{M}$, where $T\mathcal{M}$ denotes the tangent bundle, one has a system of differential equations:

$$\frac{\mathrm{d}x^j}{\mathrm{d}t} = X^j(x), \qquad x^j(0) = x_0^j. \tag{9}$$

This vector field can be represented by the differential operator[6]

$$X(x) = X^j(x)\partial_j, \tag{10}$$

where $\partial_1, \ldots, \partial_n$ is the induced coordinate basis in $T\mathcal{M}$. An integral curve of (9) defines a flow $\varphi_t : \mathcal{M} \to \mathcal{M}$. Notice that (9) has unique solutions, at least locally, since X is locally Lipschitz due to the smoothness of $\mathcal{M}$. The flow can be represented by the exponential map

$$\varphi_t = \mathrm{e}^{tX} = I + tX + \frac{1}{2}t^2X^2 + \cdots. \tag{11}$$

Through its pullback, denoted by φ_t^*, the Lie derivative of a tensor α of rank $(0, q)$ along X is defined by

$$(\mathcal{L}_X\alpha)(x) \equiv \frac{\mathrm{d}}{\mathrm{d}t}\bigg|_{t=0} \varphi_t^*\alpha(x) = \lim_{t\to 0} \frac{\varphi_t^*\alpha(\varphi_t(x)) - \alpha(x)}{t}. \tag{12}$$

The dynamical system is said to *preserve* α if and only if $\mathcal{L}_X\alpha = 0$.

Let $\phi_h : \mathbb{R}^n \to \mathbb{R}^n$ be a numerical integrator of order $r \geqslant 1$ for the system (9)—as defined in (5) and (6). Since X is locally Lipschitz, we have $\|X(y) - X(x)\| \leqslant L_X\|y - x\|$ for a constant $L_X > 0$ and for all $x, y \in \mathcal{M}$ in some region of interest. It follows from classical results [21, 22] that there exists $L_\phi > L_X$ such that we obtain control on a global error:

$$\|\phi_h^\ell(x_0) - \varphi_{t_\ell}(x_0)\| \leqslant C(\mathrm{e}^{L_\phi t_\ell} - 1)h^r, \tag{13}$$

for some constant $C > 0$ and initial state $x_0 \in \mathcal{M}$. Note that we have denoted $\phi_h^\ell \equiv \phi_h \circ \cdots \circ \phi_h$. Thus, for a fixed t_ℓ the numerical method is accurate up to order $\mathcal{O}(h^r)$. However, if t_ℓ is free the error grows exponentially. For this reason, although higher-order methods may provide accurate solutions in a short span of time, they can be inaccurate and unstable for large times.

[6] We use Einstein summation convention throughout the paper.

J. Stat. Mech. (2021) 043402

Formally, every numerical integrator ϕ_h can be seen as the *exact flow* of a modified or perturbed system [18–22, 36]:

$$\frac{\mathrm{d}x^j}{\mathrm{d}t} = \tilde{X}^j(x), \qquad \tilde{X} \equiv X + \Delta X_1 h + \Delta X_2 h^2 + \cdots, \tag{14}$$

where the ΔX's are expressed in terms of X and its derivatives. We refer to $\tilde{X}$ as the perturbed or *shadow vector field*. In general, the series in (14) is divergent, and it is necessary to consider a truncation [36]. Following [19], suppose we have found a truncation[7]

$$\tilde{X}_k = X + \Delta X_1 h + \cdots + \Delta X_k h^k \quad (k \geqslant r) \tag{15}$$

such that ϕ_h is an integrator of order k, namely $\|\phi_h(x) - \varphi_{h,\tilde{X}_k}(x)\| = \mathcal{O}(h^{k+1})$, where $\varphi_{h,\tilde{X}_k}$ denotes the exact flow of (14) with $\tilde{X}$ replaced by $\tilde{X}_k$. Define

$$\Delta X_{k+1}(x) \equiv \lim_{h\to 0} \frac{\phi_h(x) - \varphi_{h,\tilde{X}_k}(x)}{h^{k+1}}. \tag{16}$$

Then one can show that

$$\tilde{X}_{k+1} \equiv \tilde{X}_k + \Delta X_{k+1} h^{k+1} \tag{17}$$

yields a flow for which ϕ_h is an integrator of order $k+1$. Proceeding inductively, one can find higher-order vector fields $\tilde{X}_k$, with increasing k, such that $\varphi_{h,\tilde{X}_k}$ becomes closer and closer to ϕ_h. However, since (14) eventually diverges, there exists a truncation point $k^\star$ such that $\|\phi_h(x) - \varphi_{h,\tilde{X}_{k^\star}}(x)\|$ is as small as possible. Finding $k^\star$ and estimating the size of the ΔX's terms is quite technical, but it has been carried out in seminal work [18], and the approach has been further improved in subsequent literature [19, 36].

Theorem 2 (see [19]). *Assume that X is real analytic and bounded on a compact subset of its domain. Assume that the numerical method ϕ_h is real analytic of order r. Then, there exists a family of shadow vector fields $\tilde{X}$ such that*

$$\left\| X(x) - \tilde{X}(x) \right\| = \mathcal{O}(h^r), \qquad \left\| \phi_h(x) - \varphi_{h,\tilde{X}}(x) \right\| \leqslant C h e^{-r}\, e^{-h_0/h}, \tag{18}$$

where the constants $C, h_0 > 0$ do not dependent on the step size h.

This result holds in full generality, for any *autonomous* dynamical system and any numerical integrator. Next we will discuss how it becomes particularly useful in the case of conservative Hamiltonian systems.

3.2. Conservative Hamiltonian systems

Before talking about symplectic integrators, we need to introduce conservative Hamiltonian systems. Hamiltonian systems are ubiquitous because they are naturally attached

[7] Which exists for $k = r$ by assumption.

J. Stat. Mech. (2021) 043402

to the geometry of the cotangent bundle $T^*\mathcal{M}$ of any differentiable manifold $\mathcal{M}$ [16, 17]. We provide a concise introduction to key results that will be necessary later.

Definition 3. Let $\mathcal{M}$ be an even-dimensional smooth manifold supplied with a closed nondegenerate two-form ω. More precisely:

(a) $\mathrm{d}\omega = 0$;

(b) On any tangent space $T_x\mathcal{M}$, if $\omega(X, Y) = 0$ for all $Y \neq 0 \in T_x\mathcal{M}$, then $X = 0$.

Then ω is called a *symplectic structure* and $(\mathcal{M}, \omega)$ a *symplectic manifold*.

Theorem 4. *Let $q^1, \ldots, q^n$ be local coordinates of $\mathcal{M}$ and $q^1, \ldots, q^n, p_1, \ldots, p_n$ the corresponding induced coordinates of the cotangent bundle $T^*\mathcal{M}$. Then $T^*\mathcal{M}$ admits a closed nondegenerate symplectic structure,*

$$\omega = \mathrm{d}p_j \wedge \mathrm{d}q^j, \tag{19}$$

and is therefore a symplectic manifold.

Proof. There always exists a globally defined Liouville–Poincaré one-form, $\lambda \equiv p_j\,\mathrm{d}q^j \in T^*\mathcal{M}$ [16]. Applying the exterior derivative induces the Poincaré two-form $\omega \equiv \mathrm{d}\lambda = \mathrm{d}p_j \wedge \mathrm{d}q^j$. Since $d^2 = 0$ (see (A.9)) we trivially have $\mathrm{d}\omega = 0$. It is also easy to see that ω is nondegenerate; e.g. in a matrix representation $\omega = \begin{pmatrix} 0 & -I \\ +I & 0 \end{pmatrix}$. Thus $\det(\omega) = 1 \neq 0$. □

Theorem 5. *A dynamical system with phase space $T^*\mathcal{M}$ preserves the symplectic structure (19) if and only if it is (locally) a conservative Hamiltonian system, namely has the form in (2) with a time-independent Hamiltonian $H = H(q, p)$.*

Proof. Let $\gamma : \mathbb{R} \to \mathcal{M}$ be a curve parametrized by t, so that $q^j(t) \equiv (q^j \circ \gamma)(t)$ and $p_j(t) \equiv (p_j \circ \gamma)(t)$ are time-dependent coordinates over $T^*\mathcal{M}$. Consider the tangent vector $X \equiv \frac{\mathrm{d}}{\mathrm{d}t}$ to this curve, which in a coordinate basis is given by

$$X = \frac{\mathrm{d}q^j}{\mathrm{d}t}\frac{\partial}{\partial q^j} + \frac{\mathrm{d}p_j}{\mathrm{d}t}\frac{\partial}{\partial p_j}. \tag{20}$$

Note that X lives in the tangent bundle of the phase space $T^*\mathcal{M}$. The vector field X preserves (19) if and only if $\mathcal{L}_X\omega = 0$. Recalling Cartan's magic formula,

$$\mathcal{L}_X = d \circ \mathrm{i}_X + \mathrm{i}_X \circ d, \tag{21}$$

we conclude that $(d \circ \mathrm{i}_X)(\omega) = 0$. The Poincaré lemma thus implies the existence of a (local) Hamiltonian function $H : T^*\mathcal{M} \to \mathbb{R}$, such that

$$\mathrm{i}_X(\omega) = -\mathrm{d}H. \tag{22}$$

This is actually Hamilton's equation (2) in disguise; indeed, in component form we have $\mathrm{i}_X(\omega) = \dot{p}_j\,\mathrm{d}q^j - \dot{q}^j\,\mathrm{d}p_j$ which by comparison with (22) yields (2). We have just shown that a vector field that preserves the symplectic form (19) generates Hamiltonian dynamics. It is now easy to show the converse, namely that the flow of a Hamiltonian system preserves the two-form (19). Given a Hamiltonian H, we have the equations

J. Stat. Mech. (2021) 043402

of motion (2) with an associated vector field X_{H}. These equations can equivalently be written in the form (22), as already shown. Using the identities $\mathrm{d}^2 H = 0$ and $\mathrm{d}\omega = 0$ in (21) implies $\mathcal{L}_{X_{\mathrm{H}}}\omega = 0$. □

Finally, another fundamental property of Hamiltonian systems is energy conservation, which follows immediately from the equations of motion (2):

$$\frac{\mathrm{d}H}{\mathrm{d}t} = 0. \tag{23}$$

Thus, any conservative Hamiltonian system have two fundamental properties: its flow preserve the symplectic structure, and the Hamiltonian is a constant of motion.

3.3. Symplectic integrators

Consider the following class of numerical methods.

Definition 6. A numerical integrator ϕ_h for a conservative Hamiltonian system is a *symplectic integrator* if it preserves (19), i.e. $\phi_h^* \circ \omega \circ \phi_h = \omega$ where ϕ_h^* is the pullback.

It is now easy to see that the flow of the perturbed system (14) associated to a symplectic integrator also preserves ω exactly if it is Hamiltonian. As a consequence, theorem 5 implies that the perturbed system must be Hamiltonian, i.e. there exists a shadow Hamiltonian $\tilde{H}$ which is a perturbed version of H. Indeed, since ϕ_h preserves ω by assumption, and the flow of the perturbed system (14) is an exact description of ϕ_h, the shadow vector field $\tilde{X}$ obeys $\mathcal{L}_{\tilde{X}}\omega = 0$. Replacing the expansion (14) and using the linearity of the Lie derivative in the vector field implies $\mathcal{L}_{\Delta X_j}\omega = 0$ for each $j = 1, 2, \ldots$. Hence, theorem 5 implies that not only $\tilde{X}$ but all ΔX_j's are Hamiltonian vector fields. That is, by the same argument leading to (22), there exists a function $\tilde{H}$ and functions H_j's such that

$$\mathrm{i}_{\tilde{X}}(\omega) = -\mathrm{d}\tilde{H}, \qquad \mathrm{i}_{\Delta X_j}(\omega) = -\mathrm{d}H_j. \tag{24}$$

Using the series (14), combining these two equations, and using (22), we have that

$$-\mathrm{d}\tilde{H} = \mathrm{i}_X(\omega) + \sum_j h^j \mathrm{i}_{\Delta X_j}(\omega) = -\mathrm{d}H - \sum_j h^j \,\mathrm{d}H_j, \tag{25}$$

or equivalently

$$\tilde{H} = H + hH_1 + h^2 H_2 + \cdots. \tag{26}$$

Moreover, the shadow Hamiltonian $\tilde{H}$ is exactly conserved by the perturbed system, or equivalently by the symplectic integrator: $\tilde{H} \circ \phi_h = \tilde{H}$. If we now consider a truncation (17), or equivalently if we truncate (26), then the flow $\varphi_{h,\tilde{X}_k}$ exactly conserves the truncated shadow Hamiltonian $\tilde{H}_k$:

$$\tilde{H}_k \circ \varphi_{h,\tilde{X}_k} = \tilde{H}_k. \tag{27}$$

J. Stat. Mech. (2021) 043402

We are now ready to state the most important property of symplectic integrators. Adapting ideas from [18] we can prove the following.

Theorem 7. *Let ϕ_h be a symplectic integrator of order r. Assume that the Hamiltonian H is Lipschitz. Then ϕ_h conserves H up to*

$$H \circ \phi_h^\ell = H \circ \varphi_{\ell h} + \mathcal{O}(h^r), \tag{28}$$

for exponentially large times $t_\ell = \mathcal{O}(h^r e^r e^{h_0/h})$. Recall that $\varphi_{\ell h}$ is the true flow and $H = H \circ \varphi_{\ell h}$ is conserved, thus $H(q_\ell, p_\ell) = H(q_0, p_0) + \mathcal{O}(h^r)$.

Proof. Let $\tilde{X} \equiv \tilde{X}_k$ be a truncated shadow vector field associated to ϕ_h—in what follows we omit k for simplicity. We already know that (27) holds true, hence

$$\tilde{H} \circ \phi_h^\ell - \tilde{H} = \sum_{i=0}^{\ell-1} \left(\tilde{H} \circ \phi_h^{i+1} - \tilde{H} \circ \phi_h^i \right) = \sum_{i=0}^{\ell-1} \left(\tilde{H} \circ \phi_h - \tilde{H} \circ \varphi_{h,\tilde{X}} \right) \circ \phi_h^i, \tag{29}$$

where the first equality is an identity. Let $\tilde{L}$ be the Lipschitz constant of $\tilde{H}$. Using the second relation of (18) we find that

$$\left| \left(\tilde{H} \circ \phi_h^\ell - \tilde{H} \right)(x_0) \right| \leqslant \tilde{L} \sum_{i=0}^{\ell-1} \| \phi_h(x_i) - \varphi_{h,\tilde{X}}(x_i) \| \leqslant \tilde{L} C \ell h \mathrm{e}^{-r}\, \mathrm{e}^{-h_0/h}, \tag{30}$$

so ϕ_h preserves $\tilde{H}$ up to an exponentially small error in h^{-1}. In order to approximate H, write (26) in the form $\tilde{H} = H + \mathcal{O}(h^r)$—since ϕ_h has order r—to obtain (28). Note that to ensure the contribution from (30) remains smaller than $\mathcal{O}(h^r)$ we have to choose $t_\ell = h\ell$ such that $t_\ell \mathrm{e}^{-r}\, \mathrm{e}^{-h_0/h} \sim h^r$. □

Theorem 7 explains the benefits of symplectic integrators. Besides preserving the symplectic structure of the system exactly, such methods generate solutions that remain within $\mathcal{O}(h^r)$ of the true energy surface of the system and thus exhibit long-term stability. It is well-known that in practice symplectic integrators tend to outperform alternative approaches when simulating conservative Hamiltonian systems [23–25].

The situation is quite different for non-conservative or dissipative Hamiltonian systems. Even if one applies a symplectic integrator to the system written in the extended phase space, *the Hamiltonian is no longer a conserved quantity*. This conservation law is the most basic assumption underneath theorem 7; if (23) is no longer true, then (27) is no longer true, and the argument leading to (29) and (30) breaks down. Therefore, it is not guaranteed that applying a symplectic integrator to a non-conservative Hamiltonian system will closely reproduce the Hamiltonian, which is varying over time, nor is it guaranteed that the method will exhibit long-term stability. One of the main contributions of the current paper is to show that theorem 7 can be extended to general non-conservative Hamiltonian systems despite the nonexistence of such a conservation law.

J. Stat. Mech. (2021) 043402

4. Non-conservative Hamiltonian systems

Consider a time-dependent Hamiltonian $H = H(t, q, p)$[8]. The evolution of the system is still governed by Hamilton's equation (33), however the energy conservation law (23) no longer holds and is replaced by

$$\frac{\mathrm{d}H}{\mathrm{d}t} = \frac{\partial H}{\partial t}. \tag{31}$$

We begin by introducing a $(2n+1)$-dimensional extended phase space $T^*\bar{\mathcal{M}}$ in which time becomes a new coordinate, so that $q^0 = t, q^1, \ldots, q^n, p_1, \ldots, p_n$ are local coordinates of $T^*\bar{\mathcal{M}}$. The evolution of the system is now generated by the vector field

$$X \equiv X^\mu \partial_\mu = \frac{\partial}{\partial q^0} + \frac{\mathrm{d}q^j}{\mathrm{d}s}\frac{\partial}{\partial q^j} + \frac{\mathrm{d}p_j}{\mathrm{d}s}\frac{\partial}{\partial p_j}, \tag{32}$$

where $\mu = 0, 1, \ldots, n$, $X^0 = 1$, and s denotes the 'new time parameter'. Thus, the *non-autonomous* Hamiltonian system (2) is equivalent to the autonomous system

$$\frac{\mathrm{d}q^0}{\mathrm{d}s} = 1, \qquad \frac{\mathrm{d}q^j}{\mathrm{d}s} = \frac{\partial H}{\partial p_j}, \qquad \frac{\mathrm{d}p_j}{\mathrm{d}s} = -\frac{\partial H}{\partial q^j}, \tag{33}$$

over $T^*\bar{\mathcal{M}}$, where $H = H(q^0, \ldots, q^n, p_1, \ldots, p_n)$ is independent of s. Importantly, $T^*\bar{\mathcal{M}}$ is odd-dimensional so *this phase space is no longer a symplectic manifold*.

We thus introduce another dimension by adding a conjugate momentum p_0 that pairs with $q^0 = t$. To make the distinction clear, we denote the $(n+1)$-dimensional configuration manifold by $\hat{\mathcal{M}} \equiv \mathbb{R} \times \mathcal{M}$, which has local coordinates $q^0, \ldots, q^n$. The associated cotangent bundle $T^*\hat{\mathcal{M}}$ is now of even dimensionality $2n+2$, with coordinates $q^0, \ldots, q^n, p_0, \ldots, p_n$. Therefore, $T^*\hat{\mathcal{M}}$ has a natural Liouville–Poincaré one-form $\Lambda = p_\mu \mathrm{d}q^\mu$ which, as in the proof of theorem 4, induces a closed nondegenerate Poincaré two-form:

$$\Omega \equiv \mathrm{d}\Lambda = \mathrm{d}p_\mu \wedge \mathrm{d}q^\mu. \tag{34}$$

This makes $T^*\hat{\mathcal{M}}$ a proper *symplectic manifold*. Requiring that the vector field

$$Y \equiv Y^\mu \partial_\mu = \frac{\mathrm{d}q^\mu}{\mathrm{d}s}\frac{\partial}{\partial q^\mu} + \frac{\mathrm{d}p_\mu}{\mathrm{d}s}\frac{\partial}{\partial p_\mu} \tag{35}$$

preserves the symplectic structure (34) implies—by the argument leading to (22)—that

$$\mathrm{i}_Y \Omega = -\mathrm{d}\mathscr{H} \tag{36}$$

for some Hamiltonian $\mathscr{H}: T^*\hat{\mathcal{M}} \to \mathbb{R}$. In components, we have the following Hamilton's equations:

$$\frac{\mathrm{d}q^0}{\mathrm{d}s} = \frac{\partial \mathscr{H}}{\partial p_0}, \qquad \frac{\mathrm{d}p_0}{\mathrm{d}s} = -\frac{\partial \mathscr{H}}{\partial q^0}, \qquad \frac{\mathrm{d}q^j}{\mathrm{d}s} = \frac{\partial \mathscr{H}}{\partial p_j}, \qquad \frac{\mathrm{d}p_j}{\mathrm{d}s} = -\frac{\partial \mathscr{H}}{\partial q^j}, \tag{37}$$

[8] As probably evident by now, we often refer to 'dissipative' Hamiltonian systems although the reader should keep in mind that everything we say actually holds for any explicitly time-dependent or non-conservative Hamiltonian system.

J. Stat. Mech. (2021) 043402

where $j = 1, \ldots, n$ are spatial indexes. Moreover, since now $\mathscr{H}$ does not depend explicitly on time s, the above system is actually conservative:

$$\frac{\mathrm{d}\mathscr{H}}{\mathrm{d}s} = 0. \tag{38}$$

At this stage, the higher-dimensional system (37) is not equivalent to (33). In order to create this equivalence we need to impose constraints, which means *fixing a gauge*. Note that the symplectic form (34) is $\Omega = \mathrm{d}p_0 \wedge \mathrm{d}q^0 + \omega$, where ω is the symplectic form (19) for the original phase space $T^*\mathcal{M}$. Requiring the vector fields (35) and (32) to be the same, and using (36) together with (22), yields

$$0 = \mathrm{i}_Y\Omega + \mathrm{d}\mathscr{H} = \mathrm{i}_X\mathrm{d}p_0 \wedge \mathrm{d}q^0 + \mathrm{i}_X\omega + \mathrm{d}\mathscr{H} = \mathrm{d}(-p_0 - H + \mathscr{H}). \tag{39}$$

Thus, up to an irrelevant constant, we must have

$$\mathscr{H}(q^0, \ldots, q^n, p_0, \ldots, p_n) = p_0 + H(q^0, \ldots, q^n, p_1, \ldots, p_n). \tag{40}$$

Note that we carefully made the variable dependencies of each term explicit. This equation defines an *embedded submanifold* in the symplectic manifold $T^*\hat{\mathcal{M}}$. Hence, the dynamics of the non-conservative Hamiltonian system (32) lies on a hypersurface of constant energy $\mathscr{H}$. More precisely, from (40) the first equation in (37) gives

$$\frac{\mathrm{d}q^0}{\mathrm{d}s} = 1, \tag{41}$$

which together with the two last equations of (37) becomes precisely the original system (33) over the extended phase space $T^*\bar{\mathcal{M}}$. The second equation of (37) reproduces the dissipation given by (31):

$$\frac{\mathrm{d}p_0}{\mathrm{d}s} = -\frac{\partial H}{\partial q^0} = -\frac{\mathrm{d}H}{\mathrm{d}s}, \tag{42}$$

where the second equality follows from (38) together with (40). Hence, up to another irrelevant constant, we have

$$p_0(s) = -H(s), \tag{43}$$

with $H(s) = H(q(s), p(s))$. Note that in (43) the Hamiltonian is solely a function of time—the actual trajectories have been replaced—therefore p_0 is completely fixed.

We remark that (41) and (43) are specific choices of coordinates on $T^*\hat{\mathcal{M}}$ which remove the spurious degrees of freedom that are not present in the original system. This procedure of embedding the phase space of the non-conservative Hamiltonian system (33), which does not admit a symplectic structure, into a higher-dimensional symplectic manifold is called *symplectification* [16, 17]. We provide an illustration in figure 1.

Let us comment on another point behind the gauge choice (41) and (43). On the extended phase space $T^*\bar{\mathcal{M}}$ it is still possible to distinguish between position q^0 and momentum p_0. The flow $\varphi_s = \mathrm{e}^{sX}$ defines orbits $s \mapsto q^\mu(s)$ on $\hat{\mathcal{M}}$. Such orbits are considered equivalent by time reparametrization, $s \mapsto s'(s)$. However, to match the original orbits of the time-dependent Hamiltonian system over $\mathcal{M}$, one must fix $s = q^0 = t$. This

J. Stat. Mech. (2021) 043402

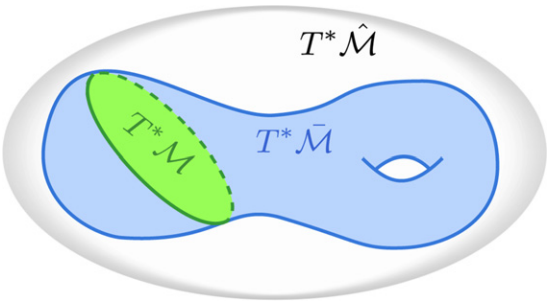

Figure 1. The symplectification consists of the embeddings $T^*\mathcal{M} \hookrightarrow T^*\bar{\mathcal{M}} \hookrightarrow T^*\hat{\mathcal{M}}$, each of dimension $2n$, $2n+1$, and $2n+2$, respectively. The original dissipative (or non-conservative) Hamiltonian system has phase space $T^*\mathcal{M}$. When the system is written in autonomous form it has phase space $T^*\bar{\mathcal{M}}$, which is a presymplectic manifold that can naturally be embedded as a submanifold of constant energy $\mathscr{H} = 0$ in the symplectic manifold $T^*\hat{\mathcal{M}}$, which can be associated to the phase space of a conservative Hamiltonian system.

means *fixing a reference frame* on $T^*\bar{\mathcal{M}}$. For this reason, time-dependent Hamiltonian systems are not covariant and one *is not free to reparametrize the original time* t. In other words, since the Hamiltonian system is explicitly time-dependent, time transformations are not canonical.

4.1. Presymplectic manifolds

We are now in a position to delineate the specific geometry underlying non-conservative Hamiltonian systems. First, we introduce a useful generalization of symplectic manifolds [16].

Definition 8. Let $\mathcal{M}$ be a differentiable manifold of dimension $(2n+\bar{n})$, $\bar{n} \geqslant 0$, supplied with a two-form ω of rank $2n$ everywhere. Then ω is called a *presymplectic form* and $(\mathcal{M}, \omega)$ a *presymplectic manifold*.

When $\bar{n} = 0$ this definition reduces to that of a symplectic manifold, and when $\bar{n} = 1$ it reduces to the definition of a *weak contact manifold*. A weak contact manifold supplied with a one-form ϑ obeying $\vartheta \wedge (\mathrm{d}\vartheta)^n \neq 0$ is a *contact manifold* [16, 17]. There is an alternative theory of contact manifolds that are intimately related to symplectic manifolds. In particular, they correspond to a particular case of presymplectic manifolds and can naturally be embedded as hypersurfaces in their symplectification, which is a symplectic manifold in $2n+2$ dimensions that is associated to $\mathcal{M}$. Furthermore, in appendix B we show that a (non-autonomous) generalization of the so-called conformal Hamiltonian systems [32] also corresponds to a particular case of the time-dependent Hamiltonian formalism discussed above.

In order to project the symplectic form (34) into the hypersurface defined by (40) we can simply substitute the gauge choice $q^0 = t$ and $p_0 = -H$ to obtain

$$\Omega = -\mathrm{d}H \wedge \mathrm{d}t + \omega, \tag{44}$$

J. Stat. Mech. (2021) 043402

where we recall that ω is the original symplectic form of $T^*\mathcal{M}$. Moreover, the equations of motion (36) reduce to

$$\mathrm{i}_X\Omega = 0, \qquad \mathrm{i}_X \mathrm{d}t = 1. \tag{45}$$

The vector field X, whose flow $\varphi_s = \mathrm{e}^{sX}$ generates dynamical evolution on $\hat{\mathcal{M}}$, is thus a *zero mode* of Ω. Note that, from Cartan's formula (21), if we require that a vector field X obeys (45), then it immediately implies $\mathcal{L}_X\Omega = 0$ so that Ω is preserved. The symplectic form Ω is closed, however when projected into $T^*\bar{\mathcal{M}}$ it becomes *degenerate*. One can see this through a matrix representation [37]:

$$\Omega = \left(\begin{array}{c|cc} 0 & 0 & 0 \\ \hline 0 & 0 & -I \\ 0 & +I & 0 \end{array}\right) \tag{46}$$

which has a vanishing determinant. Therefore, the phase space of a non-conservative or dissipative Hamiltonian system written in the autonomous form (33) is a presymplectic manifold (see again figure 1).

4.2. Presymplectic integrators

Since a non-conservative system (33) admits a symplectification, we can construct structure-preserving discretizations by imposing constraints on a *symplectic integrator*. More precisely, we can apply any standard symplectic integrator to the higher-dimensional conservative system (37). Then by the gauge choice in (41) and (43) we obtain an integrator for system (33). Such a method will preserve a presymplectic structure. Accordingly, we refer to such integrators as *presymplectic integrators*.

Definition 9. A numerical map ϕ_h is a *presymplectic integrator* for a non-conservative Hamiltonian system if it is obtained from a symplectic integrator for its symplectification under the gauge fixing (43) and (41).

Since the Hamiltonian $\mathscr{H}$ of the higher-dimensional system (37) is conserved, we can apply standard results for symplectic integrators to derive conclusions about presymplectic integrators and thereby derive properties of systems without an underlying conservation law.

Theorem 10. *A presymplectic integrator ϕ_h of order r preserves the explicitly time-dependent Hamiltonian (assumed to be Lipschitz) up to*

$$H \circ \phi_h^\ell = H \circ \varphi_{\ell h} + \mathcal{O}(h^r), \tag{47}$$

for exponentially large simulation times $s_\ell = h\ell = \mathcal{O}(h^r e^r\, e^{h_0/h})$.

Proof. Let $\Phi_h : \mathbb{R}^{2n+2} \to \mathbb{R}^{2n+2}$ be a symplectic integrator for the high-dimensional Hamiltonian system (37). Since $\mathscr{H}$ is conserved, theorem 7 implies

$$\mathscr{H} \circ \Phi_h^\ell = \mathscr{H} \circ \Psi_{\ell h} + \mathcal{O}(h^r), \tag{48}$$

with $s_\ell = \mathcal{O}(h^r \mathrm{e}^r\, \mathrm{e}^{h_0/h})$ and where Ψ_s denotes the true flow. With the gauge choice (41) and (43) the system is projected into the hypersurface (40), thus Ψ_s reduces to φ_s, which

J. Stat. Mech. (2021) 043402

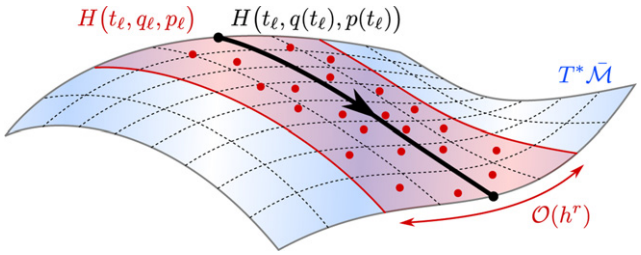

Figure 2. A presymplectic integrator closely preserves the time-dependent Hamiltonian; theorem 10. The numerical trajectories lie on the same presymplectic manifold as the non-conservative system and the numerical value $H(t_\ell, q_\ell, p_\ell)$ exhibits a small and bounded error of size $\mathcal{O}(h^r)$ with respect to the true value $H(t_\ell, q(t_\ell), p(t_\ell))$.

is the true flow of (33), and Φ_h reduces to $\phi_h : \mathbb{R}^{2n+1} \to \mathbb{R}^{2n+1}$, which approximates φ_s. Thus, using these maps together with the substitution of (40) into (48), we conclude:

$$H \circ \phi_h^\ell + p_0(\ell h) = H \circ \varphi_{\ell h} + p_0(\ell h) + \mathcal{O}(h^r). \tag{49}$$

It is important to recall that p_0 is a fixed function of time and this is why it can be canceled on both sides to give (47). □

Theorem 10 is an extension of theorem 7 to non-conservative Hamiltonian systems. The numerical solutions provided by presymplectic integrators are thus within a small and bounded error $\mathcal{O}(h^r)$ from the hypersurface (40); see figure 2 for an illustration. Hence, in the case of dissipative systems, whatever convergence or decaying properties the system may have, a presymplectic integrator will closely reproduce its behavior.

In appendix C we provide a detailed step-by-step procedure for constructing presymplectic integrators. The procedure is straightforward, essentially involving an application of symplectic integrators with a natural choice for incorporating the time variable. We now turn to the consequences of theorem 10 to dissipative systems.

5. Preserving rates and stability of dissipative systems

Let us consider how presymplectic integrators can be used to construct 'rate-matching' discretizations. We consider a standard optimization problem (1) and study dissipative systems obtained from the Hamiltonian (3), which we repeat here for convenience:

$$H = \mathrm{e}^{-\eta_1(t)} T(t, q, p) + \mathrm{e}^{\eta_2(t)} f(q) \tag{50}$$

where η_1, η_2 are positive and nondecreasing. These functions are responsible for introducing dissipation in the system. Recall that we assume the kinetic energy T is Lipschitz continuous. Given a specific system, suppose that a convergence rate $f(q(t)) - f(q^\star)$ as described in (4) is known, where $f(q^\star)$ is a minimum of f in a neighborhood of the initial

J. Stat. Mech. (2021) 043402

conditions. We are now able to prove theorem 1 stated in the introduction as a corollary of theorem 10.

Proof of Theorem 1. Replacing (50) into (47), where we now fix $s = t$, yields

$$f(q_\ell) \leqslant f(q(t_\ell)) + \mathrm{e}^{-\eta_1(t_\ell)-\eta_2(t_\ell)} \left\{T\left(t_\ell, q(t_\ell), p(t_\ell)\right) - T\left(t_\ell, q_\ell, p_\ell\right)\right\} + Kh^r \mathrm{e}^{-\eta_2(t_\ell)} \tag{51}$$

for all $t_\ell = \mathcal{O}(h^r \mathrm{e}^r \mathrm{e}^{h_0/h})$ and some constant $K > 0$. Recall that q_ℓ and $q(t_\ell)$ are the discrete- and continuous-time trajectories, respectively. Let L_T be the Lipschitz constant of the kinetic energy T. Substituting the global error (13) into the second term gives

$$|f(q_\ell) - f(q(t_\ell))| \leqslant h^r \mathrm{e}^{-\eta_2(t_\ell)} \left(K + L_T C(\mathrm{e}^{L_\phi t_\ell} - 1)\mathrm{e}^{-\eta_1(t_\ell)}\right). \tag{52}$$

We thus conclude that

$$f(q_\ell) = f(q(t_\ell)) + \mathcal{O}\left(h^r \mathrm{e}^{-\eta_2(t_\ell)}\right) \tag{53}$$

provided

$$(\mathrm{e}^{L_\phi t} - 1)\mathrm{e}^{-\eta_1(t)} < \infty \tag{54}$$

for all sufficiently large t. □

Therefore, under suitable conditions, presymplectic integrators reproduce the continuous-time rates of convergence of dissipative Hamiltonian systems. We make several remarks:

- As mentioned earlier, the assumptions of theorem 1 are mild; the kinetic energy being Lipschitz is naturally satisfied in a range of applications, and the Lipschitz condition (7) is also satisfied for a large class of integrators. The underlying reason is because $\mathcal{M}$ is a smooth manifold.
- We used a conservative global error (13) to bound the kinetic term in (51). A specialized analysis may yield a better bound, which could allow condition (54) to be relaxed. However, this would have to be justified by a dedicated backward error analysis.
- Increasing the order of accuracy r influences (53) in a beneficial way. However, the error is dominated by $\mathrm{e}^{-\eta_2}$ which suggests that in this optimization context using higher-order integrators may not be of significant practical importance. That said, higher-order methods tend to be more stable so there may be other benefits.
- Interestingly, the error in (53) is even smaller than the error in approximating the Hamiltonian (47), thanks to the function η_2. If η_2 grows just enough, this error may become completely negligible, even for large step sizes and integrators of low order.
- We recall that the restriction $t_\ell = h\ell \sim h^r \mathrm{e}^r \mathrm{e}^{h_0/h}$ may be irrelevant. To give an idea, with $r = 1$, $h_0 = 1$, and $h = 0.1$ we have $\ell \sim 6 \times 10^4$, and with $h = 0.01$ we have $\ell \sim 10^{43}$. These are sufficiently large iteration numbers for most practical purposes.

Note that theorem 1 is a consequence of theorem 10, which previously was known to hold only for conservative systems. The implications are similar to those of the conservative case. Indeed, the reason why presymplectic integrators are able to closely reproduce the time-dependent Hamiltonian is because—as in the conservative case—they exactly

J. Stat. Mech. (2021) 043402

preserve a shadow Hamiltonian, despite being non-conservative. This is important physically since, in principle, the Hamiltonian contains all the information one may wish to extract about the system. In particular, our result implies that such methods closely preserve the *energy* as well—which is not the Hamiltonian since it depends explicitly on time. For instance, within the generalized conformal Hamiltonian formalism discussed in appendix B, the 'physical energy' and 'physical momenta' are given by

$$\mathcal{E}\left(q, p_{\text{mech}}\right) = \mathrm{e}^{-\eta(t)} H(t, q, p), \quad p_{\text{mech}} = \mathrm{e}^{-\eta(t)} p. \tag{55}$$

Note that, in contradistinction to H, the energy $\mathcal{E}$ *does not depend explicitly on time*. Thus, since presymplectic integrators closely preserve H, they also closely preserve $\mathcal{E}$. This provides another perspective on the result expressed in theorem 1. Indeed, if for a particular system we have that $\mathcal{E} \geqslant 0$ and $\dot{\mathcal{E}} \leqslant 0$, then $\mathcal{E}$ is also a *Lyapunov function*[9]. Once a Lyapunov function is available, one can deduce stability properties of the system around critical points. Therefore, since presymplectic integrators also reproduce the behavior of the Lyapunov function—through H—they faithfully reproduce the phase portrait and the stability of critical points. Moreover, the *decaying rate* of $\mathcal{E}$ will also be numerically imitated and this is another way of seeing why such methods are 'rate-matching'. We stress that these ideas correspond to a dissipative generalization of what is known to hold true for structure-preserving integrators of conservative systems, in which case $\mathcal{E} = H$ is constant.

5.1. The choice of damping

Let us comment on some consequences of the condition (54) which can impose some limitations. There are two ways to satisfy it. The first is if the method converges quickly so that $\mathrm{e}^{L_\phi t_\ell - \eta_1(t_\ell)}$ remains bounded regardless of η_1, or equivalently we enforce $t_\ell \leqslant \bar{t}$, where $\bar{t}$ is a solution to

$$L_\phi \bar{t} - \eta_1(\bar{t}) \leqslant C \tag{56}$$

for some constant $C > 0$. The second way to satisfy (54) is if η_1 grows fast enough, allowing t_ℓ to be arbitrarily large. For instance, setting

$$\eta_1(t) = \gamma t \tag{57}$$

for some constant $\gamma \geqslant L_\phi$ suffices for all $t \geqslant 0$. Curiously, this choice implies constant damping and can be related to the heavy-ball method [15]—see also [5] for details[10].

As an alternative, from (54) we have

$$\left(1 + L_\phi t + \frac{1}{2}(L_\phi t)^2 + \cdots\right) \mathrm{e}^{-\eta_1(t)} < \infty, \tag{58}$$

[9] As a concrete example, consider (70) below with $\eta_1 = \eta_2 = \eta(t)$. The physical energy is given by $\mathcal{E} = (1/2)\dot{q} \cdot M\dot{q} + f(q)$, and with $p_{\text{mech}} = M\dot{q} = \mathrm{e}^{-\eta(t)} p$ we have $\mathcal{E} = \mathrm{e}^{-\eta(t)} H$. In this case $\mathcal{E} \geqslant 0$ and $\mathrm{d}\mathcal{E}/\mathrm{d}t = -\dot{\eta}\, \dot{q} \cdot M\dot{q} \leqslant 0$ (assuming that M is symmetric and positive semidefinite).

[10] With $\eta_1 = \eta_2 = \gamma t$ and $T = \frac{1}{2}\|p\|^2$ into (50) the equations of motion give $\ddot{q} + \gamma\dot{q} = -\nabla f(q)$, which is a nonlinear generalization of the damped harmonic oscillator. The heavy-ball method [15] is actually a structure-preserving—conformal symplectic—discretization of this system [5].

J. Stat. Mech. (2021) 043402

which is satisfied if $(L_\phi t)^m \mathrm{e}^{-\eta_1(t)} < \infty$ for all powers m, i.e. $\eta_1(t) \sim m \log(L_\phi t)$. Thus one can choose

$$\eta_1(t) = \gamma \log t \tag{59}$$

with a suitable $\gamma > 0$ to ensure that (58) holds up to some high-order term. Also curiously, the choice (59) is related to the damping of Nesterov's method [14] which attains the optimal convergence rate for convex functions f[11].

Note that the choice (59) can guarantee (58) only up to a finite power m, thus we are on the edge of violating this condition—in fact we are formally violating it but in practice this may yield a viable algorithm. On the other hand, the choice (57) may be overkill. It may be reasonable to consider an intermediate alternative:

$$\eta_1(t) = \gamma_1 \log t + \gamma_2 t^\delta \tag{60}$$

for constants $0 < \delta \leqslant 1$ and $\gamma_1, \gamma_2 > 0$. With this choice the condition on the mth term in the series (58) becomes $L_\phi^m t^{m-\gamma_1} \mathrm{e}^{-\gamma_2 t^\delta} < \infty$, which can be guaranteed even if $\gamma_1 < m$ with suitable choices of γ_2 and δ.

Summing up, presymplectic integrators are able to match the continuous-time rates provided the condition (54) is satisfied, which involves an appropriate choice of damping. If the system is overdamped this condition is more likely to hold, however the system would tend to be slower. On the other hand, if the damping is weak the system tends to be fast, but at the cost of violating (54). We thus see the tradeoff is delicate and is problem-dependent in general, given that L_ϕ in (54) is related to the Lipschitz constant of the original vector field which depends on the potential $f(q)$.

6. Bregman dynamics

Given that the Bregman Hamiltonian [2] provides a general framework for deriving continuous-time optimization procedures, we consider this case in some detail. The Hamiltonian has the form

$$H = \mathrm{e}^{\alpha+\gamma} \left\{ D_{h^\star}(\nabla h(q) + \mathrm{e}^{-\gamma} p, \nabla h(q)) + \mathrm{e}^{\beta} f(q) \right\}, \tag{61}$$

where α, β, and γ are all functions of time t, and required to satisfy the following scaling conditions:

$$\frac{\mathrm{d}\beta}{\mathrm{d}t} \leqslant \mathrm{e}^{\alpha}, \qquad \frac{\mathrm{d}\gamma}{\mathrm{d}t} = \mathrm{e}^{\alpha}. \tag{62}$$

The kinetic energy in (61) is given in terms of the Bregman divergence,

$$D_h(y, x) \equiv h(y) - h(x) - \langle \nabla h(x), y - x \rangle, \tag{63}$$

which is nonnegative for a given convex function $h : \mathcal{M} \to \mathbb{R}$. Recalling the definition of the convex dual, $h^\star$ of h, defined by the Legendre–Fenchel transformation

[11] Choosing $\eta_1 = \eta_2 = \gamma \log t$ yields the differential equation $\ddot{q} + \frac{\gamma}{t}\dot{q} = -\nabla f(q)$. Nesterov's method can be seen as a discretization of this system [1, 5].

J. Stat. Mech. (2021) 043402

$$h^\star(p) \equiv \sup_v \left\{\langle p, v\rangle - h(v)\right\}, \tag{64}$$

one can show that Hamilton's equations are given by[12]

$$\dot{q} = \mathrm{e}^{\alpha}\left\{\nabla h^*\left(\nabla h(q) + \mathrm{e}^{-\gamma}p\right) - q\right\}, \tag{65a}$$

$$\dot{p} = -\mathrm{e}^{\alpha+\gamma}\nabla^2 h(q)\left\{\nabla h^*\left(\nabla h(q) + \mathrm{e}^{-\gamma}p\right) - q\right\} + \mathrm{e}^{\alpha}p - \mathrm{e}^{\alpha+\beta+\gamma}\nabla f(q). \tag{65b}$$

In the case where f is convex, the convergence rate of this system is given by [2]

$$f(q(t)) - f(q^\star) = \mathcal{O}\left(\mathrm{e}^{-\beta(t)}\right). \tag{66}$$

Moreover, for a given α, the optimal rate is obtained with $\dot{\beta} = \mathrm{e}^{\alpha}$, thus $\beta = \gamma + C$, for some constant C, and both are determined in terms of α. We thus have:

$$f(q(t)) - f(q^\star) = \mathcal{O}\left(\mathrm{e}^{-\beta(t)}\right), \quad \beta(t) = \int^t \mathrm{e}^{\alpha(t')}\mathrm{d}t', \quad \gamma(t) = \beta(t) + C. \tag{67}$$

A choice considered by [2] is

$$\alpha = \log c - \log t, \qquad \beta = c\log t + C, \qquad \gamma = c\log t, \tag{68}$$

with $c > 0$, whereby the convergence rate (67) becomes the polynomial $\mathcal{O}\left(t^{-c}\right)$. Another possibility is

$$\alpha = \log c, \qquad \beta = ct, \qquad \gamma = ct + C, \tag{69}$$

leading to an exponential rate of $\mathcal{O}(\mathrm{e}^{-ct})$.

6.1. Separable case

To consider a case where the Bregman Hamiltonian is separable, let us start with the choice $h(x) = \frac{1}{2}x \cdot Mx$ with a symmetric positive semidefinite matrix M so that $h^\star(x) = \frac{1}{2}x \cdot M^{-1}x$ and the Bregman divergence is given by $D_{h^*}(y, x) = \frac{1}{2}(y - x) \cdot M^{-1}(y - x)$. In this case the Hamiltonian (61) takes the following form:

$$H = \frac{1}{2}\mathrm{e}^{-\eta_1(t)}p_i(M^{-1})^{ij}p_j + \mathrm{e}^{\eta_2(t)}f(q) \tag{70}$$

where we defined

$$\eta_1 \equiv \gamma - \alpha, \qquad \eta_2 \equiv \alpha + \beta + \gamma. \tag{71}$$

The quadratic kinetic energy is standard in classical mechanics and we see that M plays the role of a mass matrix. We thus have the equations of motion

$$\dot{q} = \mathrm{e}^{-\eta_1(t)}M^{-1}p, \qquad \dot{p} = -\mathrm{e}^{\eta_2(t)}\nabla f(q). \tag{72}$$

[12] Equivalently, one can write the second-order differential equation.

$$\ddot{q} + \left(\mathrm{e}^{\alpha} - \dot{\alpha}\right)\dot{q} + \mathrm{e}^{2\alpha+\beta}\left[\nabla^2 h\left(q + \mathrm{e}^{-\alpha}\dot{q}\right)\right]^{-1}\nabla f(q) = 0.$$

We see that α basically controls the damping, while $2\alpha + \beta$ increases the strength of the force $-\nabla f$. Both play a major role in the stability of the system, and they are not independent since $\dot{\beta} \leqslant \mathrm{e}^{\alpha}$.

J. Stat. Mech. (2021) 043402

One can now use any presymplectic integrator to simulate such a dissipative system—see appendix C. Because the Hamiltonian (70) is separable, standard approaches yield explicit methods which are convenient in practice. Assuming that we use a presymplectic integrator of order r, theorem 1 tells us that the continuous-time rate of convergence will be preserved:

$$\begin{aligned} f(q_\ell) - f^\star &= \mathcal{O}\left(\mathrm{e}^{-\beta(t_\ell)}\right) + \mathcal{O}\left(h^r \mathrm{e}^{-\alpha(t_\ell)-2\beta(t_\ell)}\right) \\ &\sim \mathrm{e}^{-\beta(t_\ell)}\left(1 + h^r \mathrm{e}^{-\alpha(t_\ell)-\beta(t_\ell)}\right) \\ &\sim \mathrm{e}^{-\beta(t_\ell)} \end{aligned} \tag{73}$$

provided η_1 as defined in (71) obeys the condition (54).

We present two explicit methods. Using the presymplectic Euler method given by (C.2), which has order $r = 1$, we obtain the following updates:

$$\begin{aligned} p_{\ell+1} &= p_\ell - h\mathrm{e}^{\eta_2(t_\ell)}\nabla f(q_\ell), \\ t_{\ell+1} &= t_\ell + h, \\ q_{\ell+1} &= q_\ell + h\mathrm{e}^{-\eta_1(t_\ell)} M^{-1} p_{\ell+1}. \end{aligned} \tag{74}$$

This algorithm requires only one gradient computation per iteration. In a similar way, using the presymplectic leapfrog method (C.7), which has order $r = 2$, we have:

$$\begin{aligned} p_{\ell+1/2} &= p_\ell - (h/2)\mathrm{e}^{\eta_2(t_\ell)}\nabla f(q_\ell), \\ t_{\ell+1} &= t_\ell + h, \\ q_{\ell+1} &= q_\ell + (h/2)\left(\mathrm{e}^{-\eta_1(t_\ell)} + \mathrm{e}^{-\eta_1(t_{\ell+1})}\right) M^{-1} p_{\ell+1/2}, \\ p_{\ell+1} &= p_{\ell+1/2} - (h/2)\mathrm{e}^{\eta_2(t_{\ell+1})}\nabla f(q_{\ell+1}). \end{aligned} \tag{75}$$

This method also only requires one gradient computation per iteration—the last one can be reused in the subsequent iteration—but it is more accurate and stable than (74). Note also that similarly to (74) and (75) we can consider (C.4) and (C.9), respectively, which yield adjoint methods to the ones above. One can now choose any suitable scaling functions in (71) and substitute into either (74) or (75) to obtain a specific optimization algorithm.

6.2. Nonseparable case

We turn to the case of a nonseparable Hamiltonian, where the integrators considered thus far yield implicit updates that require solving nonlinear equations. This not only increases the computational burden but can affect the numerical stability. In particular, for the Bregman Hamiltonian (61), we need a construction suited to nonseparable cases. In order to obtain *explicit* methods, motivated by [38] we introduce extra degrees of freedom. Thus, given a Hamiltonian $H(t, q, p)$, we double its degrees of freedom by introducing an augmented Hamiltonian:

$$\bar{H}(t, q, p, \bar{t}, \bar{q}, \bar{p}) \equiv H(t, q, \bar{p}) + H(\bar{t}, \bar{q}, p) + \frac{\xi}{2}\left(\|q - \bar{q}\|^2 + \|p - \bar{p}\|^2\right). \tag{76}$$

J. Stat. Mech. (2021) 043402

Here $\xi > 0$ is a coupling constant that controls the strength of the last term, which forces $q = \bar{q}$ and $p = \bar{p}$[13]. The presymplectic structure of this system is now

$$\Omega = -\mathrm{d}H \wedge \mathrm{d}t + \mathrm{d}p_j \wedge \mathrm{d}q^j - \mathrm{d}H \wedge \mathrm{d}\bar{t} + \mathrm{d}\bar{p}_j \wedge \mathrm{d}\bar{q}^j. \tag{77}$$

Hamilton's equations, obtained from (76), will preserve Ω. The equations of motion are equivalent to those of the original system when $q = \bar{q}$, $p = \bar{p}$ and $t = \bar{t}$. We thus propose the numerical maps

$$\phi_h^A \begin{pmatrix} t \\ q \\ p \\ \bar{t} \\ \bar{q} \\ \bar{p} \end{pmatrix} = \begin{pmatrix} t \\ q \\ p - h\nabla_q H(t, q, \bar{p}) \\ \bar{t} + h \\ \bar{q} + h\nabla_{\bar{p}} H(t, q, \bar{p}) \\ \bar{p} \end{pmatrix}, \qquad \phi_h^B \begin{pmatrix} t \\ q \\ p \\ \bar{t} \\ \bar{q} \\ \bar{p} \end{pmatrix} = \begin{pmatrix} t + h \\ q + h\nabla_p H(\bar{t}, \bar{q}, p) \\ p \\ \bar{t} \\ \bar{q} \\ \bar{p} - h\nabla_{\bar{q}} H(\bar{t}, \bar{q}, p) \end{pmatrix}, \tag{78}$$

and

$$\phi_h^C \begin{pmatrix} t \\ q \\ p \\ \bar{t} \\ \bar{q} \\ \bar{p} \end{pmatrix} = \frac{1}{2} \begin{pmatrix} 2t \\ q + \bar{q} + \cos(2\xi h)(q - \bar{q}) + \sin(2\xi h)(p - \bar{p}) \\ p + \bar{p} - \sin(2\xi h)(q - \bar{q}) + \cos(2\xi h)(p - \bar{p}) \\ 2\bar{t} \\ q + \bar{q} - \cos(2\xi h)(q - \bar{q}) - \sin(2\xi h)(p - \bar{p}) \\ p + \bar{p} + \sin(2\xi h)(q - \bar{q}) - \cos(2\xi h)(p - \bar{p}) \end{pmatrix}. \tag{79}$$

A presymplectic integrator for any (nonseparable) time-dependent Hamiltonian system can then be constructed by composing these maps. For instance, the Strang composition given by

$$\phi_{h/2}^A \circ \phi_{h/2}^B \circ \phi_h^C \circ \phi_{h/2}^B \circ \phi_{h/2}^A \tag{80}$$

is known to generate a method of order $r = 2$—this is the same composition as the leapfrog. Note that the maps (78) and (79) are completely explicit in all variables and this approach works for any time-dependent Hamiltonian.

In particular, for the Bregman Hamiltonian (61) it suffices to substitute the gradients $\dot{q} = \nabla_p H$ and $\dot{p} = -\nabla_q H$ from (65) into (78) and (79), followed by the composition (80). This yields an explicit, second-order integrator for the general Bregman dynamics. Thanks to theorem 1, this generates an optimization algorithm that may closely preserve the continuous rate of convergence (66) for suitable functions α, β and γ.

7. Numerical experiments

The purpose of this section is twofold. First, we aim to investigate the claim of theorem 10—our main result regarding structure-preserving integrators for non-conservative

[13] It is not necessary to introduce the same term for t and $\bar{t}$ since they will be equal thanks to (41). The constant ξ has to be carefully tuned in practice; see [38] for details.

J. Stat. Mech. (2021) 043402

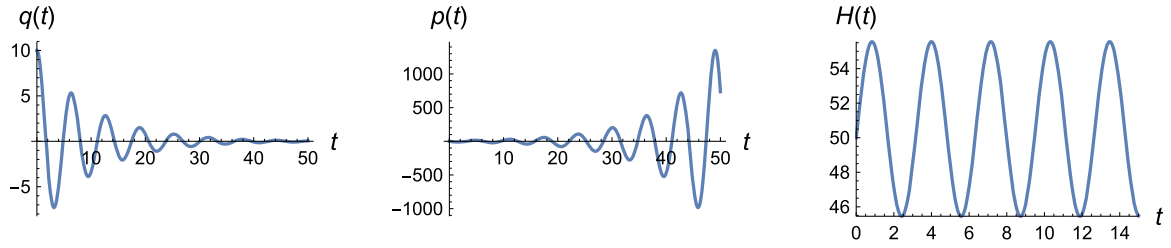

Figure 3. Exact solution (82) with $\gamma = 0.2$ and $q_0 = 10$. We replaced the actual trajectory and momentum into the Hamiltonian, which varies with time and is not conserved.

Hamiltonian systems—numerically. Second, we illustrate that our approach can form the basis for constructing reliable optimization methods based on dissipative Hamiltonian dynamics according to theorem 1.

7.1. Error growth in the Hamiltonian

In order to verify theorem 10 we need to consider cases where an exact analytical solution is available. Thus, consider the Hamiltonian (70) with $M = I$ for simplicity and with the one-dimensional potential $f(q) = q^2/2$ (higher-dimensional quadratic functions can be treated similarly by decoupling the degrees of freedom into normal modes). First, choose $\eta_1 = \eta_2 = \gamma t$ so Hamilton's equations become the damped harmonic oscillator:

$$\ddot{q} + \gamma \dot{q} + q = 0. \tag{81}$$

The exact solution of the initial value problem with $q(0) = q_0$ and $p(0) = 0$ is given by

$$q(t) = q_0 \mathrm{e}^{-t\gamma/2} \left(\cos\left(\frac{\omega t}{2}\right) + \frac{\gamma}{\omega} \sin\left(\frac{\omega t}{2}\right) \right), \qquad p(t) = -\frac{2q_0}{\omega} \mathrm{e}^{t\gamma/2} \sin\left(\frac{\omega t}{2}\right), \tag{82}$$

where $\omega \equiv \sqrt{4 - \gamma^2}$. A plot of these functions as well as the Hamiltonian is in figure 3.

We numerically integrate the equations of motion using the presymplectic Euler method (74), the presymplectic leapfrog (75), and a method of order $r = 4$ based on the Suzuki–Yoshida construction (C.12) with (75) as the base method. All of these integrators obtain accurate estimates of $q(t)$ and $p(t)$. In figure 4 (left) we show the error in the numerical estimate of the Hamiltonian over a sufficiently large simulation time. Note that this error remains bounded. To verify (47) in more detail, we fix a simulation time and vary the step size to compute the maximum error

$$\max_{\ell} |H(t_\ell, q(t_\ell), p(t_\ell)) - H(t_\ell, q_\ell, p_\ell)| \tag{83}$$

over the entire history of the system—each simulation uses a fixed step size h. We report the results for this problem in figure 4 (right). As we can see, the relation (47) is satisfied precisely.

As a second example, consider the one-dimensional potential $f(q) = q^2/2$ but now with damping functions $\eta_1 = \eta_2 = \gamma \log(t + 1)$. We thus have an harmonic oscillator with

J. Stat. Mech. (2021) 043402

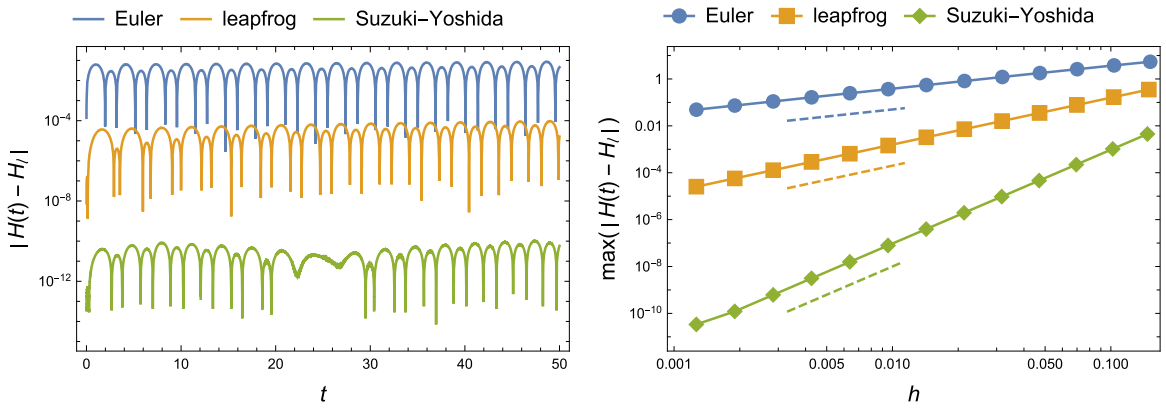

Figure 4. Error in the non-conserved Hamiltonian using the exact solution (82) and numerical estimates with presymplectic integrators. (Left) $|H(t_\ell) - H_\ell|$ (in log scale) for $t_{\max} = 50$ and $\ell_{\max} = 3 \times 10^4$ iterations, thus a step size $h = t_{\max}/\ell_{\max}$. We choose $\gamma = 0.2$ as in figure 3. We use the presymplectic Euler (74), the leapfrog (75), and the Suzuki–Yoshida (C.12) with the latter as the base method. The error remains bounded over time even though the Hamiltonian is not conserved. (Right) Under the same setting, we perform several simulations during a time interval $t \in [0, 10]$ with different step sizes h and calculate (83). The dashed lines were generated independently to verify the errors $\mathcal{O}(h)$, $\mathcal{O}(h^2)$ and $\mathcal{O}(h^4)$, respectively.

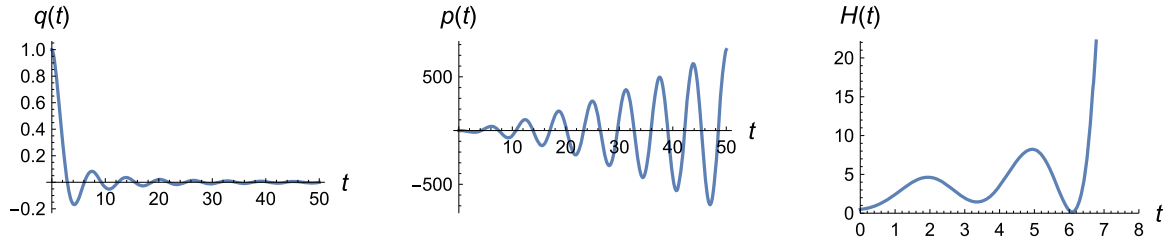

Figure 5. Exact solution (85) with $\gamma = 3$ and $q_0 = 1$. We replaced the position and momentum into the Hamiltonian which oscillates and grows very fast with t.

decaying damping:

$$\ddot{q} + \frac{\gamma}{t+1}\dot{q} + q = 0. \tag{84}$$

The exact solution of this system with initial conditions $q(0) = q_0$ and $p(0) = 0$ is

$$\begin{aligned} q(t) &= \frac{q_0\pi}{2}(t+1)^{-\alpha_-}\left(J_{\alpha_+}(1)Y_{\alpha_-}(t+1) - Y_{\alpha_+}(1)J_{\alpha_-}(t+1)\right), \\ p(t) &= \frac{q_0\pi}{2}(t+1)^{\alpha_+}\left(Y_{\alpha_+}(1)J_{\alpha_+}(t+1) - J_{\alpha_+}(1)Y_{\alpha_+}(t+1)\right), \end{aligned} \tag{85}$$

where $\alpha_\pm \equiv (\gamma \pm 1)/2$ and J_α, Y_α denote Bessel functions of the first and second kinds, respectively. A plot of these functions together with the Hamiltonian is in figure 5.

J. Stat. Mech. (2021) 043402

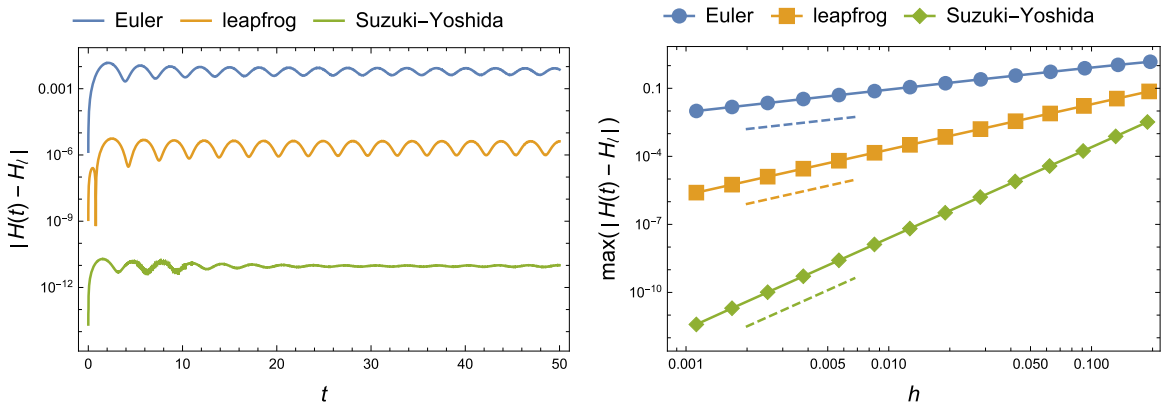

Figure 6. Error in the non-conserved Hamiltonian. (Left) $|H(t_\ell) - H_\ell|$ (in log scale) for $t_{\max} = 50$ and $\ell_{\max} = 3 \times 10^4$ (step size $h = t_{\max}/\ell_{\max}$). We choose $\gamma = 3$ as in figure 5. (Right) For each choice of step size, we compute (83) over $t \in [0, 10]$. The dashed lines are independent plots to verify the errors $\mathcal{O}(h)$, $\mathcal{O}(h^2)$, and $\mathcal{O}(h^4)$, respectively, as predicted in (47).

Using the same integrators as in the previous case, we obtain the results shown in figure 6. Again, relation (47) is verified perfectly. As expected, the leapfrog (75) is more stable than the Euler method (74), since it has order $r = 2$; however, the method based on Suzuki–Yoshida is even more stable and accurate than both (as expected since it has order $r = 4$). Let us mention that we also implemented their adjoint integrators as well, i.e. methods based on (C.4), (C.9) and (C.12); the results were essentially the same.

For comparison, let us consider Nesterov's method—a well-known optimization algorithm in the literature—that corresponds to a discretization of the Hamiltonian system (72) with $M = I$. Nesterov's method is provably a first-order integrator however it is not structure-preserving [5]. By considering the same setting as that of figure 4, we obtain the results shown in figure 7 (left). Note how Nesterov's has a *growing error* in the Hamiltonian, in contrast to the presymplectic leapfrog which we include as a reference. Moreover, in figure 7 (right) we introduce *excitation* in the system by choosing instead $\gamma = -1$. Note how the presymplectic leapfrog still closely reproduces the Hamiltonian, i.e. up to a bounded error $\mathcal{O}(h^r)$, in agreement with theorem 10 which holds not only for dissipative systems but also for general non-conservative systems. We also conducted numerical experiments in the case of system (84) with similar results.

7.2. Quadratic programming

Consider minimizing a random quadratic function in the unconstrained case:

$$\min_q \left\{ f(q) \equiv \frac{1}{2} q \cdot Mq \right\}, \tag{86}$$

where $M = \frac{1}{n} A^{\mathrm{T}} A$, with A an $r \times n$ matrix, $r/n \to y$ for some $0 < y \leqslant 1$, and where the entries A^{ij} are sampled from a standard normal distribution—we set $n = 1000$ and $y = 0.8$ in our example. Thus M has rank r and its eigenvalues are distributed according

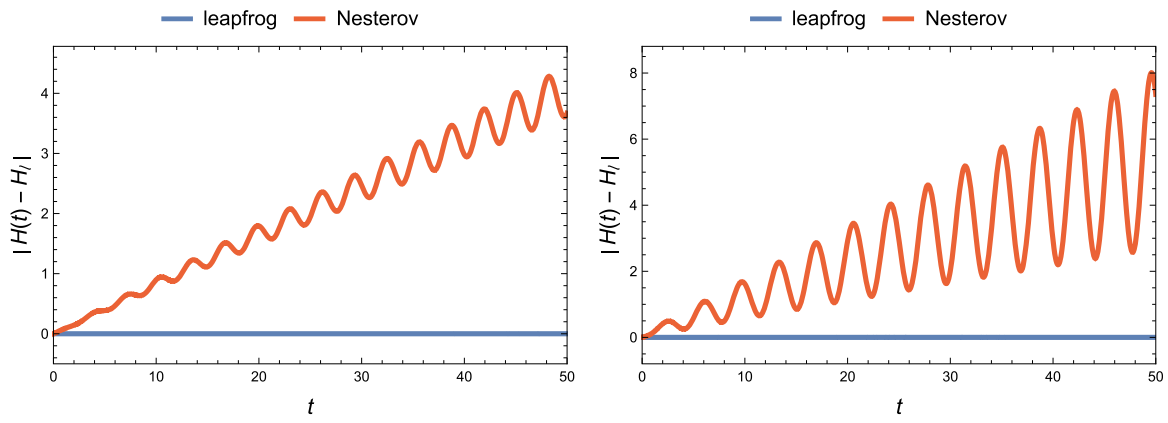

Figure 7. Contrary to our structure-preserving (presymplectic) integrators, Nesterov's method has an unbounded error in the Hamiltonian. (Left) use exactly the same setting as in figure 4. (Right) We choose $\gamma = -1$ so that we 'inject' energy into the system; note that a presymplectic method closely preserves—up to a bounded error $\mathcal{O}(h^r)$—general time-dependent Hamiltonians (not only for dissipative systems) in agreement with theorem 10.

to the Marchenko–Pastur law. We solve problem (86) with the presymplectic leapfrog method (75) and compare it with Nesterov's accelerated method. We consider a constant damping $\eta_1 = \eta_2 = \gamma t$ for both methods.

We thus generate 50 random functions of the kind (86) and use these algorithms with appropriate choice of parameters (γ, h). Their convergence rates are illustrated in figure 8 where we plot the mean of $\|\nabla f(q_\ell)\|$ against the iteration number ℓ (the shaded areas correspond to $\pm$ one standard deviation). Note that in this case the dissipative version of the leapfrog was faster due to a larger choice of step size; we stress that both methods have similar performance, the difference is that structure-preserving discretizations tend to be more stable and thus may accept larger step sizes for sufficiently well-behaved problems. To verify the stability of these methods more closely, in figure 9 we show a γ–h phase diagram of $\|\nabla f\|$ using a single sample of the random function (86); i.e. for each choice (γ, h) we run both algorithms for a certain maximum number of iterations ($\ell_{\max} = 800$) or until a small tolerance on $\|\nabla f\|$ is attained (we choose 10^{-3}). A light color means a small value of $\|\nabla f\|$ such that the algorithm converges successfully (the lighter the smallest value of the gradient), while a dark color means larger values of $\|\nabla f\|$ (black means complete failure). Note how the method based on the leapfrog is indeed more stable since it admits a wider light color region; i.e. it converges successfully under a wider range of step sizes. By a closer inspection of this figure we can also see that Nesterov's method introduces some spurious damping since it converges in some cases even when $\gamma = 0$.

7.3. Learning the Ising model with Boltzmann machines

To further illustrate the feasibility of our approach to optimization, we consider a more realistic problem. Consider the two-dimensional (ferromagnetic) Ising model whose

J. Stat. Mech. (2021) 043402

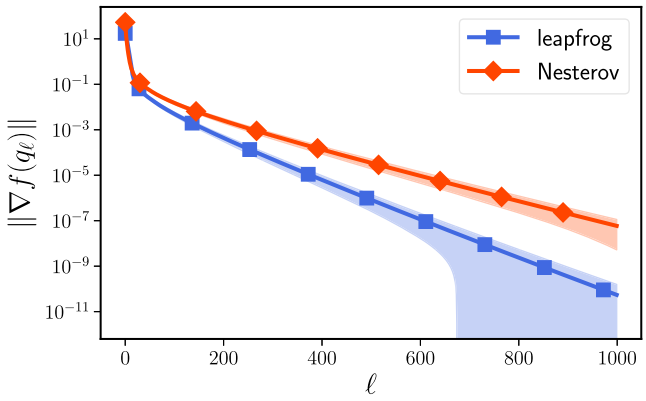

Figure 8. We perform 50 Monte Carlo runs when minimizing (86) with presymplectic leapfrog (75) and Nesterov's method. We choose $\gamma = 0.7$ for both and step size $h = 0.9$ for leapfrog whereas $h = 0.5$ for Nesterov—these were the largest values such that these methods converged on all trials. Solid lines are the mean of $\|\nabla f\|$ and shaded areas $\pm\sigma$ (standard deviation).

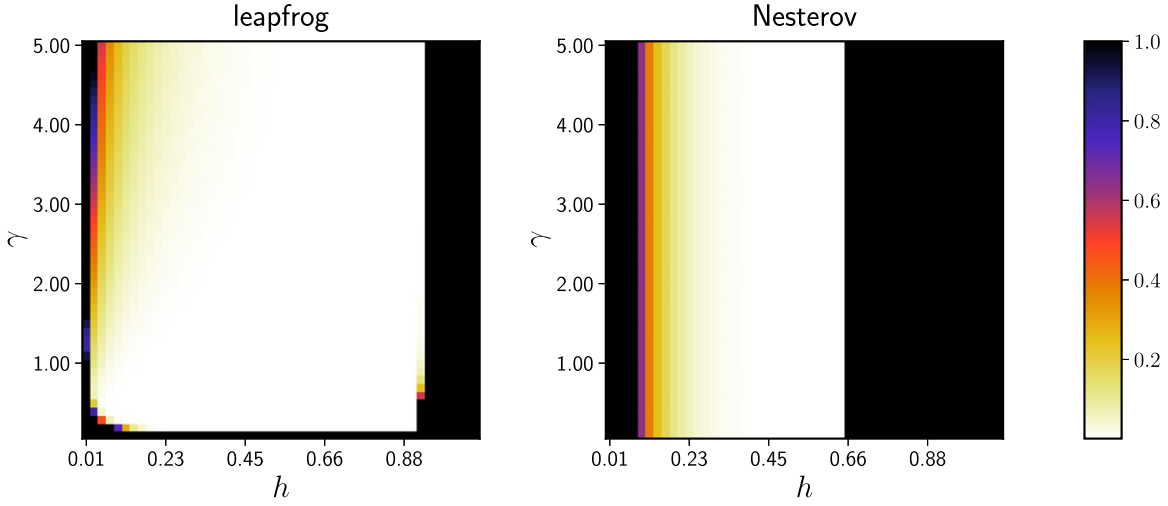

Figure 9. Phase diagram of $\|\nabla f\|$ in terms of (γ, h). Dark color means large $\|\nabla f\|$ so that the algorithm diverged (we truncated larger values to 1 for visualization purposes). Note the wider area in light color for presymplectic leapfrog which illustrates its improved stability.

Hamiltonian is given by

$$H \equiv -\sum_{\langle ij \rangle} \sigma_i \sigma_j, \tag{87}$$

where the spin variables take values $\sigma_i = \pm 1$. Onsager (1944) solved this system analytically. This system undergoes a second-order phase transition at the critical temperature

$T_c = 2/\log(1+\sqrt{2}) \approx 2.27$. The canonical partition function is

$$Z \equiv \sum_{\{\sigma_i\}} e^{-\beta H}, \tag{88}$$

with inverse temperature $\beta \equiv 1/T$, from which any thermodynamic property of the system can be computed, including the average energy and heat capacity:

$$\langle E\rangle = -\frac{\partial \log Z}{\partial \beta}, \qquad \langle C\rangle = \frac{\partial \langle E\rangle}{\partial T} = \frac{\langle E^2\rangle - \langle E\rangle^2}{T^2}. \tag{89}$$

We want to 'learn' the canonical distribution $\rho = e^{-\beta H}/Z$ using a generative model known as *restricted Boltzmann machine* (RBM)—such an approach has recently attracted significant interest in physics [39–42]. Briefly, an RBM is a neural network with two layers, the so-called *visible* layer which has a number of neurons equal to the dimensionality of the input data vector, and the *hidden* layer which can have an arbitrary number of neurons. These two layers are connected with each other through parameters ('weights') that we collectively denote by q (neurons in the same layer are not connected). Given training data—e.g. admissible states of the Ising model at a given temperature T—an RBM is trained by minimizing a 'loss function' $f(q)$ which can be seen as an energy function that depends on the weights of the network. The gradient of this loss function can be approximated via a technique called contrastive divergence [43], which involves running a Markov chain for k steps. In practice, a simple *gradient descent* method is often used in RBM's [39, 42]. After the RBM is trained, it provides a statistical representation of the probability distribution of the data, thus allowing us to sample the canonical distribution and estimate thermodynamic quantities such as (89). Naturally, to train the RBM we need generate data, which can done by simulating the Ising model with a Monte Carlo method.

Following [39, 42], we consider the Ising model on a lattice of size $N = 8 \times 8$ and periodic boundary conditions. We generate 10^5 Ising configurations using a standard Monte Carlo simulation with the Metropolis algorithm; we use N^3 equilibration steps for several values of the temperature in the range $T \in [0.5, 4.5]$. Then, for each temperature T, we feed 2×10^3 random samples of these states to the RBM which is optimized with gradient descent and the presymplectic leapfrog method (75) (with $M = I$ for simplicity). For gradient descent we use a step size $h = 5 \times 10^{-3}$ while for the leapfrog we let $h = 2.5 \times 10^{-2}$ and set the damping coefficient γ according to $\mu \equiv e^{-\gamma h/2}$ with $\mu = 0.98$ (these values were chosen via a rough grid search). To compute (stochastic) gradients we use a 'batch size' of 100 and run these algorithms for 2×10^3 iterations. The number of neurons in the hidden layer of the RBM is set to be 400 and we use only one step $k = 1$ in the contrastive gradient computation (more steps yield better results but are computationally demanding). The RBM estimates for the energy and specific heat are reported in figure 10[14]. Note that the presymplectic leapfrog (75) yields improvements over gradient descent. Indeed, to illustrate its faster convergence, in figure 11 we show a plot of the loss function during training for a single temperature; analogous results

[14] These results can be compared with [39, 42] where more extensive (and expensive) experiments were performed for this same problem.

J. Stat. Mech. (2021) 043402

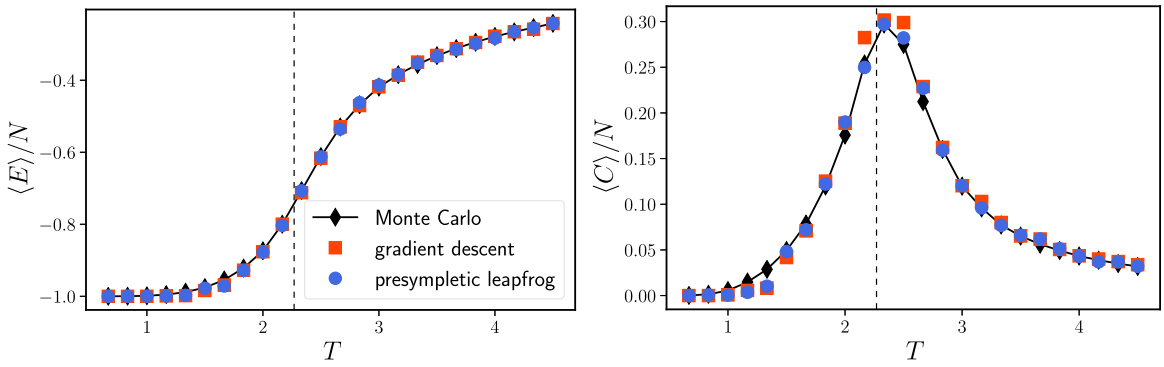

Figure 10. Learning a 2D Ising model (8×8 lattice) with a RBM trained with gradient descent (standard approach) and the presymplectic leapfrog method (75). The RBM was trained with only 2×10^3 data points. We include a comparison with the Metropolis Monte Carlo estimates to the average energy and heat capacity (89) using 10^5 configurations. The vertical dashed line indicates the theoretical value of the critical temperature $T_c \approx 2.27$.

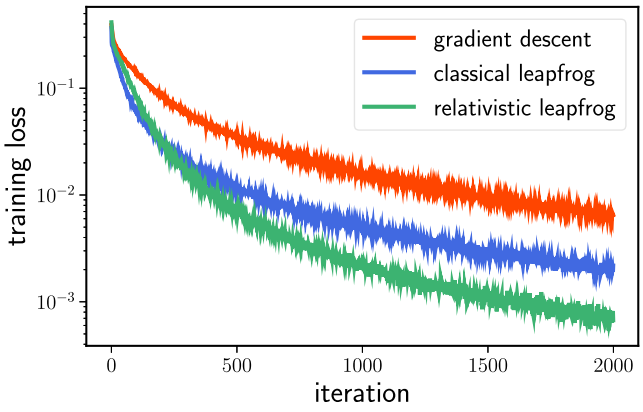

Figure 11. Convergence rate in training an RBM with gradient descent and the presymplectic leapfrog method (75) for one data point ($T \approx 2.83$) of figure 10. We also include results for a method obtained from a dissipative relativistic system (90).

hold for other values. We also tested Nesterov's method on this problem and the results were essentially the same as the ones reported for the presymplectic leapfrog.

Finally, to illustrate that different physical systems can also lead to feasible optimization methods, we consider the presymplectic leapfrog (C.9) with a relativistic kinetic energy. That is, we consider the following Hamiltonian (see appendix B and [5]):

$$H = \mathrm{e}^{\gamma t}\sqrt{\mathrm{e}^{-2\gamma t}c^2 p^j p_j + m^2c^4} + \mathrm{e}^{\gamma t} f(q). \tag{90}$$

We set $m = 1$, $h = 2.8 \times 10^{-2}$, $\mu = \mathrm{e}^{-\gamma h/2} = 0.99$ and we fix the speed of light to $c = 5$—in the algorithm c can be considered a free parameter that controls the kinetic energy. In figure 11 we see that this method has faster convergence compared to the

J. Stat. Mech. (2021) 043402

classical system. (We also considered the entire curves of figure 10 but the results were not significantly different from the classical case.)

8. Discussion

We have introduced '*presymplectic integrators*' as a class of discretizations that are suitable for simulating explicitly time-dependent or non-conservative—and in particular dissipative—Hamiltonian systems. This framework accommodates a large class of dissipative dynamical systems that are appropriate for applications in optimization and machine learning. We have also shown that, besides preserving the underlying *presymplectic geometry* of non-conservative Hamiltonian systems, these methods nearly preserve the Hamiltonian and exhibit long-term stability despite the absence of a conservation law; see theorem 10. This extends into non-conservative settings the most important property of symplectic integrators which are restricted to conservative systems. Thus, our approach and theoretical conclusions are applicable to a variety of scientific disciplines where the simulation of non-conservative or dissipative systems play an important role, such as nonequilibrium statistical physics, thermodynamics of open systems, complex and nonlinear systems, economics, and so forth.

Focusing on optimization, we showed that, for a general class of dissipative systems arising from a Hamiltonian in the form (3), presymplectic integrators are able to preserve the continuous-time rates of convergence up to a negligible error, as long as certain conditions are satisfied; see theorem 1. This provides a systematic and first-principles approach to deriving 'rate-matching' discretizations, thereby obviating the need for a discrete-time convergence analysis[15]. As a concrete example, we considered the Bregman Hamiltonian, providing general methods from which specific optimization algorithms can be derived, in both the separable and the nonseparable case. Our theoretical conclusions and the feasibility of this approach were also well-supported by numerical experiments.

We comment on some problems that might deserve further study. First, we showed that condition (54) is essential and in particular leads to the damping strategies (57) and (59) related to the heavy ball and Nesterov's method, respectively. We also argued that a more elaborate choice (60) may be beneficial. Thus, finding the *optimal damping* for a given class of problems and relating to the amount of energy being dissipated seems an interesting problem. More generally, finding physical systems that may provide a faster convergence is interesting—we considered the relativistic kinetic energy besides the classical one but other choices may be possible. Second, it would be appealing to find numerical schemes with a better global error—see equation (7)—or obtain improved bounds for existing methods, since this would automatically relax the condition (54). Finally, our geometric construction is fully general and one can also consider the simulation of dissipative systems on arbitrary (smooth) curved manifolds. Thus, our framework can also be used to solve optimization problems over a Riemannian manifold by including the appropriate metric in the kinetic part of the Hamiltonian.

[15] Of course, if one wants to study fine details of a specific algorithm's performance, a discrete analysis, together with an appropriate backward error analysis, may be necessary.

J. Stat. Mech. (2021) 043402

Acknowledgments

We wish to thank Jelena Diakonikolas and Michael Muehlebach for helpful discussions. This work was supported by grant ARO MURI W911NF-17-1-0304.

Appendix A. Background on differential geometry

In this section we provide a brief overview of those elements of differential geometry that we need for our results. For a fuller presentation we refer to any of the excellent textbooks on the subject (e.g. [16, 17, 37, 44, 45]).

Let $\mathcal{M} \equiv \mathcal{M}^n$ be a smooth n-dimensional manifold. Let $p \in \mathcal{M}$ and $(\mathcal{U}, x)$ be a *chart* so that p can be assigned local coordinates, $x(p) \equiv (x^1(p), \dots, x^n(p))$ in $\mathbb{R}^n$. The coordinates x and the point p are used interchangeably, and we often refer to the former to indicate a point on the manifold. To each $x \in \mathcal{M}$ there is an associated vector space $T_x\mathcal{M}$ called the *tangent space*. The coordinates x induces a basis $\partial_1, \dots, \partial_n$ in $T_x\mathcal{M}$, where $\partial_j \equiv \frac{\partial}{\partial x^j}$. Thus, $V|_x = V^j(x)\partial_j$ is a representation of the vector $V|_x \in T_x\mathcal{M}$[16]. The collection of all tangent vectors of $\mathcal{M}$ form the *tangent bundle* $T\mathcal{M}$. One can then represent a (contravariant) vector field by the differential operator

$$V(x) \equiv V^j(x)\partial_j, \tag{A.1}$$

which can be seen as a cross section of the tangent bundle $T\mathcal{M}$. For a given x, the vector field V assigns a single vector, $V(x) = V|_x$. Note that a point in $T\mathcal{M}$ has $2n$ coordinates, $x^1, \dots, x^n, V^1, \dots, V^n$.

To each $V|_x$ there is an associated dual vector, $\alpha|_x : T_xM \to \mathbb{R}$; i.e. α is a linear functional. Dual vectors are called covectors or one-forms and they live on the *cotangent space* denoted by $T_x^*\mathcal{M}$, which is isomorphic to $T_x\mathcal{M}$. The collection of all one-forms at every point of $\mathcal{M}$ forms the *cotangent bundle* $T^*\mathcal{M}$. The coordinate basis x induces a dual basis $\mathrm{d}x^1, \dots, \mathrm{d}x^n$ in $T_x^*\mathcal{M}$, defined by $\mathrm{d}x^j(\partial_k) = \partial_k(\mathrm{d}x^j) = \delta_k^j$, where δ is the Kronecker delta. Similarly to (A.1) one can now represent a one-form field $\alpha \in T^*\mathcal{M}$ as

$$\alpha(x) = \alpha_j(x)\mathrm{d}x^j, \tag{A.2}$$

which is a cross section of the cotangent bundle $T^*\mathcal{M}$. The action of dual vectors is thus $\alpha(V)|_x = V(\alpha)|_x = \alpha_j(x)V^j(x)$. Note that $T^*\mathcal{M}$ is a $2n$-dimensional space where a point has coordinates $x^1, \dots, x^n, \alpha_1, \dots, \alpha_n$. The cotangent bundle $T^*\mathcal{M}$ is very special since it can be shown that it is itself a symplectic manifold (see theorem 4).

A general *tensor* T of rank (p, q) is a multilinear map $T : \bigotimes^p T_x^*\mathcal{M} \bigotimes^q T_x\mathcal{M} \to \mathbb{R}$. In a coordinate basis it is written as

$$T = T^{j_1 \dots j_p}{}_{k_1 \dots k_q} \partial_{j_1} \cdots \partial_{j_p} \mathrm{d}x^{k_1} \cdots \mathrm{d}x^{k_q}. \tag{A.3}$$

In calculations, it is useful to focus on the components $T^{j_1 \dots j_p}{}_{k_1 \dots k_q}$ alone and omit the basis altogether. A *contravariant tensor* is a tensor of rank $(p, 0)$, for some $p \geqslant 1$, and

[16] We use Einstein's summation convention throughout, where a pair of upper and lower indices are summed over; e.g. $X^j\partial_j \equiv \sum_{j=1}^n X^j\partial_j$, $\alpha_{jk}T^{\ell jk} \equiv \sum_{j=1}^n \sum_{k=1}^n \alpha_{jk}T^{\ell jk}$, etc. Upper indices denote components of vectors—also called contravariant vectors—in $T_x\mathcal{M}$, while lower indices denote components of dual vectors—also called covectors—which belong to the cotangent space $T_x^*\mathcal{M}$.

J. Stat. Mech. (2021) 043402

a *covariant tensor* is a tensor of rank $(0, q)$, for some $q \geqslant 1$. A *q-form* is a $(0, q)$-tensor which is totally *antisymmetric* in its indices. In a basis it is denoted as

$$\alpha = \frac{1}{q!}\alpha_{j_1\dots j_q}\mathrm{d}x^{j_1} \wedge \cdots \wedge \mathrm{d}x^{j_q}, \tag{A.4}$$

where $\wedge$ denotes the *exterior product*[17]. Given another p-form β, one can compose the $(p+q)$-form $\alpha \wedge \beta$ which obeys

$$\alpha \wedge \beta = (-1)^{pq}\,\beta \wedge \alpha. \tag{A.5}$$

It is useful to introduce a notation to denote the space of q-forms at x, namely $\bigwedge^q T^*_x\mathcal{M}$, and as before we obtain a bundle $\bigwedge^q T^*\mathcal{M}$ of q-form fields by allowing the coefficient $\omega_{j_1\dots j_q}(x)$ to depend on x.

Another important operation is the *exterior derivative*:

$$d\colon \bigwedge^{q} T^*\mathcal{M} \to \bigwedge^{q+1} T^*\mathcal{M}, \tag{A.6}$$

which can be defined componentwise as

$$\mathrm{d}\alpha(x) \equiv \frac{1}{q!}\frac{\partial \alpha_{j_1\dots j_q}(x)}{\partial x^k}\mathrm{d}x^k \wedge \mathrm{d}x^{j_1} \wedge \cdots \wedge \mathrm{d}x^{j_q}. \tag{A.7}$$

This is a linear operation, $\mathrm{d}(c_1\alpha + c_2\beta) = c_1\mathrm{d}\alpha + c_2\mathrm{d}\beta$, for any forms α and β. Its main properties are given by the equation

$$\mathrm{d}(\alpha \wedge \beta) = (\mathrm{d}\alpha) \wedge \beta + (-1)^q \alpha \wedge (\mathrm{d}\beta), \tag{A.8}$$

and by the identity

$$d^2 = d \circ d = 0. \tag{A.9}$$

A differential form ω is said to be *closed* if $\mathrm{d}\omega = 0$. A differential q-form ω is said to be *exact* if $\omega = \mathrm{d}\lambda$ for some $(q-1)$-form λ. Trivially, from (A.9) every exact form is closed. The *Poincaré lemma* ensures the converse, namely that every closed form is also exact[18].

Given a vector $v \in T_x\mathcal{M}$ and a q-form $\alpha \in \bigwedge^q T^*_x\mathcal{M}$, the *interior product* $i_v\alpha$ is a $(q-1)$-form defined by

$$(\mathrm{i}_v\alpha)(v_2, \dots, v_q) \equiv \alpha(v, v_2, \dots, v_q). \tag{A.10}$$

In components, this is simply the contraction $(\mathrm{i}_v\alpha)_{j_2\dots j_q} = v^k\alpha_{kj_2\dots j_q}$. The interior product is also linear and satisfies an analogous relation to (A.8):

$$\mathrm{i}_v(\alpha \wedge \beta) = (\mathrm{i}_v\alpha) \wedge \beta + (-1)^q \alpha \wedge (\mathrm{i}_v\beta). \tag{A.11}$$

Since one can only operate on elements of the same vector space, it is necessary to introduce a mapping that makes it possible to move geometric objects over the

[17] For two one-forms $\alpha, \beta \in T^*_x\mathcal{M}$ we have $(\alpha \wedge \beta)(v, w) \equiv \alpha(v)\beta(w) - \beta(v)\alpha(w)$, for $v, w \in T_x\mathcal{M}$

[18] This holds for contractible manifolds, which is the case for smooth manifolds as considered in this paper.

J. Stat. Mech. (2021) 043402

manifold. In particular, given a function $F:\mathcal{M}\to\mathcal{N}$ between two manifolds $\mathcal{M}$ and $\mathcal{N}$, for any function $g:\mathcal{N}\to\mathbb{R}$ one defines the *pushforward*—also called the differential—of $v\in T_x\mathcal{M}$ to be the vector $F_*v\in T_{F(x)}\mathcal{N}$ defined by the operation

$$(F_*v)(g)\equiv v(g\circ F). \tag{A.12}$$

The *pullback* goes in the opposite direction, i.e. given a q-form $\alpha\in T^*_{F(x)}\mathcal{N}$ we obtain the q-form $F^*\alpha\in T^*_x\mathcal{M}$ through

$$F^*\alpha(v_1,\ldots,v_q)\equiv\alpha(F_*v_1,\ldots,F_*v_q), \tag{A.13}$$

for $v_j\in T_x\mathcal{M}$, $j=1,\ldots,q$. The pullback allows us to move q-forms over the manifold. By introducing the concept of a flow, $\varphi_t:\mathcal{M}\to\mathcal{M}$ induced by a vector field X of $T\mathcal{M}$, i.e. $\varphi_t=\mathrm{e}^{tX}$, one can define the *Lie derivative* of a q-form as in (12). A flow φ_t is a diffeomorphism and thus $\varphi_t^*=(\varphi_{-t})_*$. In this case, one can consider the pullback of not only q-forms but arbitrary (p,q)-tensors. Thus, the Lie derivative of a general tensor field T can be defined by

$$\mathcal{L}_XT|_x\equiv\left.\frac{\mathrm{d}}{\mathrm{d}t}\right|_{t=0}\varphi_t^*T|_{\varphi_t(x)}. \tag{A.14}$$

Given a differentiable form ω and a vector field X, we say that X preserves ω if and only if

$$\mathcal{L}_X\omega=0. \tag{A.15}$$

From the definition (A.14) this implies

$$\varphi_t^*\omega=\omega. \tag{A.16}$$

In this sense, any map $\phi:\mathcal{M}\to\mathcal{N}$ is said to be *canonical* if it preserves ω, i.e. $\phi^*\omega=\omega$. In the case of Hamiltonian systems ω is the symplectic two-form, and Hamiltonian flows generate canonical transformations, which are symplectomorphisms.

A very useful formula is Cartan's magic formula:

$$\mathcal{L}_X\alpha=d\circ\mathrm{i}_X\alpha+\mathrm{i}_X\circ\mathrm{d}\alpha \tag{A.17}$$

for any differentiable form α. Some other useful formulas are

$$\mathcal{L}_X(\alpha\wedge\beta)=(\mathcal{L}_X\alpha)\wedge\beta+\alpha\wedge(\mathcal{L}_X\beta), \tag{A.18}$$

$$\mathcal{L}_{[X,Y]}\alpha=[\mathcal{L}_X,\mathcal{L}_Y]\alpha, \tag{A.19}$$

$$\mathcal{L}_X\circ d=\mathrm{d}\circ\mathcal{L}_x, \tag{A.20}$$

$$\mathrm{i}_{[X,Y]}=\mathcal{L}_X\circ\mathrm{i}_Y-\mathrm{i}_Y\circ\mathcal{L}_X. \tag{A.21}$$

Here, $[\mathcal{L}_X,\mathcal{L}_Y]\equiv\mathcal{L}_X\mathcal{L}_Y-\mathcal{L}_Y\mathcal{L}_X$ is the *Lie bracket*. The same definition holds for $[X,Y]=XY-YX$, and in this case one refers to $[\cdot,\cdot]$ as the *commutator* of two vector fields.

J. Stat. Mech. (2021) 043402

Appendix B. Generalized conformal Hamiltonian systems

Conformal Hamiltonian systems [32] provide an alternative approach to introducing dissipation into Hamiltonian systems. In this approach, one modifies Hamilton's equations directly by adding a linear term in the momentum. It is easy to construct structure-preserving discretizations for these systems since one can split the system into conservative and dissipative parts, then apply a standard symplectic integrator to the former, while integrating the latter exactly. This approach has been recently explored in optimization [5]. The purpose of this section is to show that a (non-autonomous) generalization of conformal Hamiltonian systems correspond to a particular case of the explicit time-dependent Hamiltonian formalism introduced in section 4. As a consequence, one can construct (generalized) conformal symplectic integrators from presymplectic integrators (see definition 9).

Consider a time-independent Hamiltonian, $H = H(q, p)$, and assume a modified form of Hamilton's equations given by

$$\frac{\mathrm{d}q^j}{\mathrm{d}t} = \frac{\partial H}{\partial p_j}, \qquad \frac{\mathrm{d}p_j}{\mathrm{d}t} = -\frac{\partial H}{\partial q^j} - \gamma(t) p_j. \tag{B.1}$$

The conformal case [32] assumes that the damping coefficient $\gamma(t) = \gamma$ is constant. In this formulation, the Hamiltonian vector field is

$$X_{\mathrm{H}} = \frac{\partial H}{\partial q^i}\frac{\partial}{\partial q^i} + \frac{\partial H}{\partial p_i}\frac{\partial}{\partial p_i}, \tag{B.2}$$

and by the same geometric approach previously discussed one can see that the equations of motion (B.1) are equivalent to

$$\mathrm{i}_{X_{\mathrm{H}}}(\omega) = -\mathrm{d}H - \gamma(t)\lambda, \tag{B.3}$$

with ω defined in (19) and where $\lambda \equiv p_j \mathrm{d}q^j$ is the Liouville–Poincaré one-form. From Cartan's formula (21) we conclude that the symplectic structure contracts as

$$\mathcal{L}_{X_{\mathrm{H}}}\omega = -\gamma(t)\omega, \tag{B.4}$$

or equivalently[19]

$$\varphi_t^*\omega = \mathrm{e}^{-\eta(t)}\omega, \qquad \eta(t) \equiv \int^t \gamma(t')\mathrm{d}t'. \tag{B.5}$$

Finally, in this setting H is the energy of the system and it dissipates as

$$\frac{\mathrm{d}H}{\mathrm{d}t} = -\gamma(t)\frac{\partial H}{\partial p_j}p_j. \tag{B.6}$$

[19] From this one concludes that the phase-space volumes contract as $\mathcal{L}_{X_{\mathrm{H}}}\mathrm{vol}^{2n} = -n\gamma(t)\mathrm{vol}^{2n}$, so that $\varphi_t^*\mathrm{vol}^{2n} = \mathrm{e}^{-nC(t)}\mathrm{vol}^{2n}$. This is a dissipative version of Liouville's theorem; note the dimension dependency.

J. Stat. Mech. (2021) 043402

We now show that generalized conformal Hamiltonian systems corresponds to a particular case of the time-dependent Hamiltonian formalism. Define the time-dependent Hamiltonian K as

$$K(t,Q,P) \equiv \mathrm{e}^{\eta(t)} H\left(Q, \mathrm{e}^{-\eta(t)} P\right), \quad Q \equiv q, \quad P \equiv \mathrm{e}^{\eta(t)} p, \tag{B.7}$$

where H is the original Hamiltonian of (B.1). Now the standard Hamilton's equations yield

$$\frac{\mathrm{d}Q^j}{\mathrm{d}t} = \frac{\partial K}{\partial P_j} = \frac{\partial H(q,p)}{\partial p_j}, \qquad \frac{\mathrm{d}P_j}{\mathrm{d}t} = -\frac{\partial K}{\partial Q^j} = -\mathrm{e}^{\eta(t)} \frac{\partial H(q,p)}{\partial q^j}, \tag{B.8}$$

which when written in terms of (q,p) are precisely (B.1). Therefore, one can construct discretizations that preserve the contraction of the symplectic form (B.4) through presymplectic integrators (see definition 9) with the explicit time-dependent Hamiltonian K.

Appendix C. Constructing presymplectic integrators

As stated in definition 9, a presymplectic integrator is a reduction of a higher-dimensional symplectic integrator under the gauge fixing (41) and (43). To follow this prescription one must perform three simple steps:

(a) Choose a *symplectic integrator*—for a conservative Hamiltonian system—and apply it to the Hamiltonian system (37). This results into updates for (q^0, p_0) and for the spatial components (q^j, p_j);

(b) Set $q^0 = t$ and ignore p_0 completely—p_0 is just the actual value of the Hamiltonian as a function of time and does not participate in the dynamics, neither in the numerical procedure;

(c) Set $s = t$.

While these formal steps make clear that we are respecting the symplectification prescription previously discussed, in practice these three steps can be reduced to the following:

- Apply any 'symplectic integrator' to the time-dependent Hamiltonian $H(t,q,p)$ in the 'natural way'. By this we mean to simply include additional updates for the time variable t with the same rule as the coordinates q.

  We will provide some explicit examples below that should make this clear.

C.1. Presymplectic Euler

For a conservative Hamiltonian system one has the following version of the symplectic Euler method which is order $r = 1$ [22] ($\ell = 0, 1, \ldots$ is the iteration number and h the

J. Stat. Mech. (2021) 043402

step size):

$$\begin{aligned} p_{\ell+1} &= p_\ell - h\nabla_q H(q_\ell, p_{\ell+1}), \\ q_{\ell+1} &= q_\ell + h\nabla_p H(q_\ell, p_{\ell+1}). \end{aligned} \tag{C.1}$$

Considering a time-dependent Hamiltonian $H(t, q, p)$, since t must be treated in the same way as the coordinates q according to the above discussion, we immediately obtain the *presymplectic Euler* method given by

$$\begin{aligned} p_{\ell+1} &= p_\ell - h\nabla_q H(t_\ell, q_\ell, p_{\ell+1}), \\ t_{\ell+1} &= t_\ell + h, \\ q_{\ell+1} &= q_\ell + h\nabla_p H(t_\ell, q_\ell, p_{\ell+1}). \end{aligned} \tag{C.2}$$

Note how we have simply added an update for t following the same structure as the update for q. There is also the adjoint of (C.1) given by [22]

$$\begin{aligned} q_{\ell+1} &= q_\ell + h\nabla_p H(q_{\ell+1}, p_\ell), \\ p_{\ell+1} &= p_\ell - h\nabla_q H(q_{\ell+1}, p_\ell). \end{aligned} \tag{C.3}$$

From this we obtain an alternative to (C.2) which is

$$\begin{aligned} t_{\ell+1} &= t_\ell + h, \\ q_{\ell+1} &= q_\ell + h\nabla_p H(t_{\ell+1}, q_{\ell+1}, p_\ell), \\ p_{\ell+1} &= p_\ell - h\nabla_q H(t_{\ell+1}, q_{\ell+1}, p_\ell). \end{aligned} \tag{C.4}$$

Both of these methods, namely (C.2) and (C.4), are of order $r = 1$. Note that for an arbitrary Hamiltonian H in general they are implicit, i.e. nonlinear equations have to be solved to obtain either $q_{\ell+1}$ or $p_{\ell+1}$. However, when the Hamiltonian is separable in the form

$$H = T(t, p) + V(t, q) \tag{C.5}$$

these methods become completely explicit in all variables resulting in cheap implementations.

C.2. Presymplectic leapfrog

One of the versions of the leapfrog method for a conservative Hamiltonian is given by [22]

$$\begin{aligned} p_{\ell+1/2} &= p_\ell - (h/2)\nabla_q H(q_\ell, p_{\ell+1/2}), \\ q_{\ell+1} &= q_\ell + (h/2)\left(\nabla_p H(q_\ell, p_{\ell+1/2}) + \nabla_p H(q_{\ell+1}, p_{\ell+1/2})\right), \\ p_{\ell+1} &= p_{\ell+1/2} - (h/2)\nabla_q H(q_{\ell+1}, p_{\ell+1/2}). \end{aligned} \tag{C.6}$$

This method is obtained by composing (C.1) and (C.3), each with step size $h/2$ and in this order. This method is symmetric and thus of order $r = 2$. For a time-dependent

Hamiltonian $H(t,q,p)$ we include appropriate updates for time and obtain the following *presymplectic leapfrog* method:

$$\begin{aligned} p_{\ell+1/2} &= p_\ell - (h/2)\nabla_q H(t_\ell, q_\ell, p_{\ell+1/2}),\\ t_{\ell+1} &= t_\ell + h,\\ q_{\ell+1} &= q_\ell + (h/2)\left(\nabla_p H(t_\ell, q_\ell, p_{\ell+1/2}) + \nabla_p H(t_{\ell+1}, q_{\ell+1}, p_{\ell+1/2})\right),\\ p_{\ell+1} &= p_{\ell+1/2} - (h/2)\nabla_q H(t_{\ell+1}, q_{\ell+1}, p_{\ell+1/2}). \end{aligned} \tag{C.7}$$

There is also the adjoint version of the leapfrog which is obtained by composing (C.3) followed by (C.1) instead, i.e. [22]

$$\begin{aligned} q_{\ell+1/2} &= q_\ell + (h/2)\nabla_p H(q_{\ell+1/2}, p_\ell),\\ p_{\ell+1} &= p_\ell - (h/2)\left(\nabla_q H(q_{\ell+1/2}, p_\ell) + \nabla_q H(q_{\ell+1/2}, p_{\ell+1})\right),\\ q_{\ell+1} &= q_{\ell+1/2} + (h/2)\nabla_p H(q_{\ell+1/2}, p_{\ell+1}). \end{aligned} \tag{C.8}$$

This leads to an alternative version of the presymplectic leapfrog given by

$$\begin{aligned} t_{\ell+1/2} &= t_\ell + h/2,\\ q_{\ell+1/2} &= q_\ell + (h/2)\nabla_p H(t_{\ell+1/2}, q_{\ell+1/2}, p_\ell),\\ p_{\ell+1} &= p_\ell - (h/2)\left(\nabla_q H(t_{\ell+1/2}, q_{\ell+1/2}, p_\ell) + \nabla_q H(t_{\ell+1/2}, q_{\ell+1/2}, p_{\ell+1})\right),\\ t_{\ell+1} &= t_{\ell+1/2} + h/2,\\ q_{\ell+1} &= q_{\ell+1/2} + (h/2)\nabla_p H(t_{\ell+1/2}, q_{\ell+1/2}, p_{\ell+1}). \end{aligned} \tag{C.9}$$

Again, in general these methods are implicit but for a separable Hamiltonian (C.5) they become completely explicit in all variables. Moreover, only one gradient computation per iteration is necessary even though these methods are of order $r = 2$.

Let us comment on a useful numerical trick. In practice, for cases such as (75), large exponentials can be numerically unstable. This can be avoided by redefining variables in the algorithm. For instance, in the case of (75) one can introduce $\tilde{p}_\ell \equiv \mathrm{e}^{-\eta_2(t_\ell)} p_\ell$ to rewrite the updates as

$$\begin{aligned} \tilde{p}_{\ell+1/2} &= \mathrm{e}^{-\Delta^{(2,2)}_{h/2}(t_\ell)}\left(\tilde{p}_\ell - (h/2)\nabla f(q_\ell)\right),\\ t_{\ell+1} &= t_\ell + h,\\ q_{\ell+1} &= q_\ell + (h/2)\left(\mathrm{e}^{\Delta^{(2,1)}_{h/2}(t_\ell)} + \mathrm{e}^{-\Delta^{(1,2)}_{h/2}(t_{\ell+1/2})}\right)\tilde{p}_{\ell+1/2},\\ \tilde{p}_{\ell+1} &= \mathrm{e}^{-\Delta^{(2,2)}_{h/2}(t_{\ell+1/2})}\tilde{p}_{\ell+1/2} - (h/2)\nabla f(q_{\ell+1}), \end{aligned} \tag{C.10}$$

where $\Delta^{(a,b)}_h(t) \equiv \eta_a(t+h) - \eta_b(t)$. Note that only finite differences appear in the exponentials which prevent very large (or small) numbers in a numerical implementation. For instance, in the case where $\eta_2 = \eta_1 = \gamma t$, which was used in the experiments of

J. Stat. Mech. (2021) 043402

section 7.3, we have the following method based on the presymplectic leapfrog:

$$\begin{aligned}\tilde{p}_{\ell+1/2} &= \mu\,(\tilde{p}_\ell - (h/2)\nabla f(q_\ell))\,,\\ q_{\ell+1} &= q_\ell + h\,\cosh\,(-\log\,\mu)\tilde{p}_{\ell+1/2},\\ \tilde{p}_{\ell+1} &= \mu\tilde{p}_{\ell+1/2} - (h/2)\nabla f(q_{\ell+1}),\end{aligned} \tag{C.11}$$

where $\mu \equiv \mathrm{e}^{-\gamma h/2}$ (we did not write the update for t which is not important if one is only interested in q, and in this case one can be even more economical by replacing the last update into the first). One thus has tuning parameters h and μ for the above method.

C.3. Higher-order methods

In [46, 47] an elegant and general approach to construct arbitrarily higher-order symplectic integrators was presented. It assumes that a base method ϕ_h of order $2r$ ($r \geqslant 1$) is given and an integrator of order $2r+2$ is then obtained by the composition

$$\phi_{\tau_0 h} \circ \phi_{\tau_1 h} \circ \phi_{\tau_0 h} \tag{C.12}$$

where

$$\tau_0 \equiv \frac{1}{2-\kappa}, \qquad \tau_1 \equiv -\frac{\kappa}{2-\kappa}, \qquad \kappa^{2r+1} \equiv 2. \tag{C.13}$$

One can start with any base method of choice, such as the leapfrog. From this new integrator of order $2r+2$ one may proceeds recursively to construct even higher-order methods.

It is straightforward to adapt this procedure to presymplectic integrators by carefully adding an update for time t. However, let us mention that the number of gradient computations of the Suzuki–Yoshida approach (C.12) grows very fast with increasing order, quickly becoming unfeasible. Moreover, the truncation error of such methods tend to be rather large, although the fourth-order method obtained from the leapfrog is competitive and interesting. (See [24] and especially [48] for an interesting discussion.)

References

[1] Su W, Boyd S and Candès E J 2016 *J. Mach. Learn. Res.* **17** 1–43
[2] Wibisono A, Wilson A C and Jordan M I 2016 *Proc. Natl Acad. Sci.* **113** E7351–8
[3] França G, Robinson D P and Vidal R 2018 A nonsmooth dynamical systems perspective on accelerated extensions of ADMM (arXiv:1808.04048)
[4] França G, Robinson D P and Vidal R 2018 ADMM and accelerated ADMM as continuous dynamical systems ICML *Proc. 35th Int. Conf. on Machine Learning* pp 1559–67
[5] França G, Sulam J, Robinson D P and Vidal R 2020 *J. Stat. Mech.* 124008
[6] Krichene W, Bayen A and Bartlett P L 2015 Accelerated mirror descent in continuous and discrete time *Advances in Neural Information Processing Systems* (New York: Curran Associates) vol 28
[7] Wilson A C, Recht B and Jordan M I 2018 A Lyapunov analysis of momentum methods in optimization (arXiv:1611.02635)
[8] Scieur D, Roulet V, Bach F and d'Aspremont A 2017 Integration methods and optimization algorithms *Advances in Neural Information Processing Systems* (New York: Curran Associates) vol 30
[9] Betancourt M, Jordan M I and Wilson A C 2018 On symplectic optimization (arXiv:1802.03653)

J. Stat. Mech. (2021) 043402

[10] Zhang J, Mokhtari A, Sra S and Jadbabaie A 2018 Direct Runge–Kutta discretization achieves acceleration *Advances in Neural Information Processing Systems* (New York: Curran Associates) vol 30
[11] Shi B, Du S S, Su W J and Jordan M I 2019 Acceleration via symplectic discretization of high-resolution differential equations *Advances in Neural Information Processing Systems* (New York: Curran Associates) vol 32
[12] Muehlebach M and Jordan M I 2019 A dynamical systems perspective on Nesterov acceleration *Proc. 36th Int. Conf. on Machine Learning* 4656–62
[13] Diakonikolas J and Jordan M I 2020 Generalized momentum-based methods: a Hamiltonian perspective (arXiv:1906.00436)
[14] Nesterov Y 1983 *Sov. Math. - Dokl.* **27** 372–6
[15] Polyak B T 1964 Some methods of speeding up the convergence of iteration methods *USSR Comput. Math. Math. Phys.* **4** 1–17
[16] Berndt R 2001 *An Introduction to Symplectic Geometry* (Providence, RI: American Mathematical Society)
[17] Aebischer B, Borer M, Kalin M and Leuenberger C 1994 *Symplectic Geometry* (Berlin: Springer)
[18] Benettin G and Giorgilli A 1994 *J. Stat. Phys.* **74** 1117–43
[19] Reich S 1999 *SIAM J. Numer. Anal.* **36** 1549–70
[20] Hairer E 1994 *Ann. Numer. Math.* **1** 107–32
[21] Leimkuhler B and Reich S 2004 *Simulating Hamiltonian Dynamics* (Cambridge: Cambridge University Press)
[22] Hairer E, Lubich C and Wanner G 2006 *Geometric Numerical Integration* (Berlin: Springer)
[23] Sanz-Serna J M 1992 *Acta Numer.* **1** 243–86
[24] McLachlan R I and Quispel G R W 2006 *J. Phys. A: Math. Gen.* **39** 5251–85
[25] Iserles A and Quispel G R W 2018 Why geometric numerical integration? *Discrete Mechanics, Geometric Integration and Lie–Butcher Series* (Berlin: Springer) pp 1–28
[26] Bhatt A, Floyd D and Moore B E 2016 *J. Sci. Comput.* **66** 1234–59
[27] Moore B E 2017 *J. Comput. Appl. Math.* **323** 1–15
[28] Bhatt A and Moore B E 2019 *J. Comput. Appl. Math.* **352** 341–51
[29] Shang X and Öttinger H C 2020 *Proc. R. Soc.* A **476** 20190446
[30] Nussle T, Thibaudeau P and Nicolis S 2019 *Eur. Phys. J.* B **92** 1–10
[31] Nussle T, Thibaudeau P and Nicolis S 2019 *Phys. Rev.* B **100** 214428
[32] McLachlan R and Perlmutter M 2001 *J. Geom. Phys.* **39** 276–300
[33] Caldirola P 1941 *Il Nuovo Cimento* **18** 393–400
[34] Kanai E 1948 *Prog. Theor. Phys.* **3** 440–2
[35] Caldeira A O and Leggett A J 1981 *Phys. Rev. Lett.* **46** 211–4
[36] Hairer E and Lubich C 1997 *Numer. Math.* **76** 441–62
[37] Sternberg S 1964 *Lectures on Differential Geometry* (Englewood Cliffs, NJ: Prentice-Hall)
[38] Tao M 2016 *Phys. Rev.* E **94** 043303
[39] Torlai G and Melko R G 2016 *Phys. Rev.* B **94** 165134
[40] Carleo G and Troyer M 2017 *Science* **355** 602–6
[41] Melko R G, Carleo G, Carrasquilla J and Cirac J I 2019 *Nat. Phys.* **15** 887–92
[42] Morningstar A and Melko R G 2018 *J. Mach. Learn. Res.* **18** 1–17
[43] Hinton G E 2002 *Neural Comput.* **14** 1771–800
[44] Arnold V I, Kozlov V V and Neishtadt A I 2006 *Mathematical Aspects of Classical and Celestial Mechanics* (Berlin: Springer)
[45] Abraham R and Marsden J E 1978 *Foundations of Mechanics* (Reading, MA: Addison-Wesley)
[46] Suzuki M 1990 *Phys. Lett.* A **146** 319–23
[47] Yoshida H 1990 *Phys. Lett.* A **150** 262–8
[48] McLachlan R I 2002 *Numer. Algorithms* **31** 233–46

J. Stat. Mech. (2021) 043402